Fraunhofer Institut
Techno- und
Wirtschaftsmathematik

W. Dörfler, O. Iliev, D. Stoyanov, D. Vassileva

On Efficient Simulation of Non-Newtonian Flow in Saturated Porous Media with a Multigrid Adaptive Refinement Solver

Berichte des Fraunhofer ITWM, Nr. 70 (2004)

ISSN 1434-9973

Bericht 70 (2004)

Die Veröffentlichungen in der Berichtsreihe des Fraunhofer ITWM können bezogen werden über:

Fraunhofer-Institut für Techno- und
Wirtschaftsmathematik ITWM
Gottlieb-Daimler-Straße, Geb. 49

67663 Kaiserslautern
Germany

Telefon: +49 (0) 6 31/2 05-32 42
Telefax: +49 (0) 6 31/2 05-41 39
E-Mail: info@itwm.fraunhofer.de
Internet: www.itwm.fraunhofer.de

Vorwort

Das Tätigkeitsfeld des Fraunhofer Instituts für Techno- und Wirtschaftsmathematik ITWM umfasst anwendungsnahe Grundlagenforschung, angewandte Forschung sowie Beratung und kundenspezifische Lösungen auf allen Gebieten, die für Techno- und Wirtschaftsmathematik bedeutsam sind.

In der Reihe »Berichte des Fraunhofer ITWM« soll die Arbeit des Instituts kontinuierlich einer interessierten Öffentlichkeit in Industrie, Wirtschaft und Wissenschaft vorgestellt werden. Durch die enge Verzahnung mit dem Fachbereich Mathematik der Universität Kaiserslautern sowie durch zahlreiche Kooperationen mit internationalen Institutionen und Hochschulen in den Bereichen Ausbildung und Forschung ist ein großes Potenzial für Forschungsberichte vorhanden. In die Berichtreihe sollen sowohl hervorragende Diplom- und Projektarbeiten und Dissertationen als auch Forschungsberichte der Institutsmitarbeiter und Institutsgäste zu aktuellen Fragen der Techno- und Wirtschaftsmathematik aufgenommen werden.

Darüberhinaus bietet die Reihe ein Forum für die Berichterstattung über die zahlreichen Kooperationsprojekte des Instituts mit Partnern aus Industrie und Wirtschaft.

Berichterstattung heißt hier Dokumentation darüber, wie aktuelle Ergebnisse aus mathematischer Forschungs- und Entwicklungsarbeit in industrielle Anwendungen und Softwareprodukte transferiert werden, und wie umgekehrt Probleme der Praxis neue interessante mathematische Fragestellungen generieren.

Prof. Dr. Dieter Prätzel-Wolters
Institutsleiter

Kaiserslautern, im Juni 2001

On Efficient Simulation of Non-Newtonian Flow in Saturated Porous Media with a Multigrid Adaptive Refinement Solver

Willy Dörfler
Institut für Angewandte Mathematik II, Universität Karlsruhe (TH),
D-76128 Karlsruhe, Germany.
doerfler@math.uni-karlsruhe.de

Oleg Iliev, Dimitar Stoyanov
Fraunhofer Institut für Techno- und Wirtschaftsmathematik (ITWM),
Europaallee 10, D-67657 Kaiserslautern, Germany.
{iliev, stoyanov}@itwm.fhg.de

Daniela Vassileva
Institute of Mathematics and Informatics, Bulgarian Academy of Sciences,
Acad. G. Bonchev str., bl. 8, BG-1113 Sofia, Bulgaria.
vasileva@math.bas.bg

Abstract

Flow of non-Newtonian fluid in saturated porous media can be described by the continuity equation and the generalized Darcy law. Efficient solution of the resulting second order nonlinear elliptic equation is discussed here. The equation is discretized by a finite volume method on a cell-centered grid. Local adaptive refinement of the grid is introduced in order to reduce the number of unknowns. A special implementation approach is used, which allows us to perform unstructured local refinement in conjunction with the finite volume discretization. Two residual based error indicators are exploited in the adaptive refinement criterion. Second order accurate discretization of the fluxes on the interfaces between refined and non-refined subdomains, as well as on the boundaries with Dirichlet boundary condition, are presented here, as an essential part of the accurate and efficient algorithm. A nonlinear full approximation storage multigrid algorithm is developed especially for the above described composite (coarse plus locally refined) grid approach. In particular, second order approximation of the fluxes around interfaces is a result of a quadratic approximation of slave nodes in the multigrid - adaptive refinement (MG-AR) algorithm. Results from numerical solution of various academic and practice-induced problems are presented and the performance of the solver is discussed.

Key words: Nonlinear multigrid, adaptive refinement, non-Newtonian flow in porous media.

1 Introduction

Numerical simulation of flow in porous media is essential for better understanding and proper control in many environmental and technological processes. Saturated flows of Newtonian fluids are described by linear elliptic equation for the pressure, and a lot of attention is paid to the development of efficient multilevel and local refinement solvers for such problems (see, for example, [1, 2, 3, 4, 5]) and references therein). At the same time, numerical algorithms for flow of non-Newtonian fluid in porous media are not so well developed. A reason for this is that the problem in this case is essentially nonlinear. Main difficulties in solving such problems are related to the (strong) nonlinearity of the coefficients, stronger local effects (compared to the linear case), and possible degeneration of the equation.
In the current work we consider a numerical algorithm, which allows to efficiently solve non-degenerating problems using a nonlinear multigrid algorithm and adaptive local mesh refinement within the multigrid procedure. The governing elliptic equation is discretized by finite volume method on cell centered, adaptively locally refined grid. Main attention is paid to the following aspects of the algorithm:

i) *Proper treatment of the slave nodes in the case of local refinement.* Currently, the basic approaches for treatment the slave nodes are based on piecewise constant, or linear, or bilinear interpolation (see [5, 6]) for details. Having in mind the importance of the accurate computation of fluxes (i.e., of Darcy velocity), we consider quadratic interpolation for the slave nodes which ensures second order approximation for the fluxes.

ii) *Investigation of the performance of different error indicators.* A large number of papers devoted to various error estimators and error indicators for linear elliptic problems were published in the last decade (see, for example, [7, 8, 9, 4, 10, 11, 12, 13, 14, 15] and references therein). Here we consider two error indicators [12, 13], and investigate numerically their performance for the nonlinear problem we specified above.

iii) *Accurate discretization in the near boundary cells in the case of Dirichlet boundary conditions.* It is wellknown that the standard discretization of an elliptic equation in such cells does not approximate the governing equation (see, e.g., [16]). It is still possible to prove second order convergence for the pressure [16], however, the flux converges with first order. There are different approaches toward increasing the accuracy, we apply the one considered in [17].

iv) *Efficient solver for the discretized equations.* Nonlinear FAS algorithm, combined with multigrid on locally refined grid is used. The last is similar to MLAT [1, 2] and

FAC [3]. Note, that for such an algorithm we have to invert an symmetric positive definite operator on each grid, even in the case of using quadratic interpolation for the slave nodes.

v) *Proper software design of the solver.* The object oriented approach has been followed. The class hierarchy corresponds with the structure of the multigrid - (adaptive) local refinement algorithm. This makes possible to couple the local discretization within the control volume with further global matrix assembly, just as in the finite elements method, gaining more flexibility with no loose in the performance.

Extensive numerical experiments are performed in order to study the developed algorithm. The following aspects of the algorithm are examined:

a) Multigrid convergence in the case of global and local refinement.

b) Order of convergence for pressure and velocities in maximum and in L_2 norms for MG and MG-LR algorithms depending on the near-boundary discretization, and on the interpolation for the slave nodes (in the case of local refinement), etc.

c) Dependence of the multigrid convergence and of the achieved accuracy on the degree of nonlinearity of the problem. Each example is solved in the linear case and in two different nonlinear cases.

d) Influence of the degeneration of the coefficients (compare Example 1 and Example 2).

e) Performance of the two considered error indicators.

The reminder of the paper is organized as follows. Section 2 concerns the governing equations and their discretization. The third section describes the multigrid procedure, the adaptive local refinement algorithm, and the error indicators used. Results from numerical experiments are presented and discussed in the fourth section. Finally, some conclusions are drawn.

2 Governing equation and single-grid solution method

The governing equation is the nonlinear second order equation

$$\sum_{d=1}^{D} \frac{\partial}{\partial x_d} \left(K_d \left| \frac{\partial p}{\partial x_d} \right|^m \frac{\partial p}{\partial x_d} \right) = f, \qquad K_d > 0, \quad m = \frac{1}{n} - 1 \geq 0, \quad D \in \{2, 3\}. \tag{1}$$

It can be obtained using the first order system consisting of the *generalized Darcy law* for single phase and the *continuity equation* [18]

$$\mathbf{u}^n = -\frac{1}{\mu_0}\mathbf{K}\boldsymbol{\nabla} p,$$
$$\boldsymbol{\nabla}\cdot\,\mathbf{u} = -f,$$

where $\mathbf{u} = (u_1, \ldots, u_D)$ is the velocity vector, the notation $\mathbf{u}^n$ stands for $\mathbf{u}^n = (u_1^n, \ldots, u_D^n)$, p is the pressure, $\mathbf{K}$ is a diagonal permeability tensor with diagonal entries $K_{dd} := \mu_0(K_d)^n$ for $d = 1, \ldots, D$ and the power n is a parameter of the medium. For example, $n < 1$ for pseudoplastic fluids such as polymers and heavy oils.

The finite volume method is used for the discretization of Eq. (1) on a Cartesian rectangular cell-centered grid (i.e., the unknowns are related to the centers of the rectangles, see Fig. 1). For brevity we consider here the two-dimensional case, but the three–dimensional case is also implemented in our solver. For the discretization in the case of local refinement we refer also to [5]. We let

$$h_2\left[a_{i+1/2,j}\frac{p_{i+1,j}-p_{ij}}{h_1} - a_{i-1/2,j}\frac{p_{ij}-p_{i-1,j}}{h_1}\right] \quad +$$

$$h_1\left[b_{i,j+1/2}\frac{p_{i,j+1}-p_{ij}}{h_2} - b_{i,j-1/2}\frac{p_{ij}-p_{i,j-1}}{h_2}\right] \qquad = h_1h_2f_{ij},$$

where the coefficients $k_d\left(\dfrac{\partial p}{\partial x_d}\right) := K_d\left|\dfrac{\partial p}{\partial x_d}\right|^m$ are approximated using arithmetic averaging

$$a_{i+1/2,j} := 0.5\big(k_{1,ij} + k_{1,i+1,j}\big), \quad b_{i,j+1/2} := 0.5\big(k_{2,ij} + k_{2,i,j+1}\big),$$

where

$$k_{1,ij} := k_1\left(\frac{p_{i+1,j}-p_{i-1,j}}{2h_1}\right), \quad k_{2,ij} := k_2\left(\frac{p_{i,j+1}-p_{i,j-1}}{2h_2}\right).$$

Note, the coefficients may be computed without averaging, as $\frac{\partial p}{\partial x_d}$ can be approximated directly on the corresponding wall, but then the convergence may be slow or the method may not converge at all (for $m \geq 1$).

Second order accurate discretization of $\frac{\partial p}{\partial x_d}$ on the boundaries with Dirichlet boundary condition is used, for example on the boundary $x_1 = 0$ the following expression is used in order to approximate $\frac{\partial p}{\partial x_1}$

$$\left.\frac{\partial p}{\partial x_1}\right|_{x_1=0} = \frac{4}{3}\,\frac{p_{1j}-p_{0j}}{h/2} - \frac{1}{3}\,\frac{p_{2j}-p_{1j}}{h} + O(h^2).$$

In the non-linear case ($m > 0$) second order accurate discretization is also ensured for $\frac{\partial p}{\partial x_d}$ in the center of the first computational volume , for example

$$\left.\frac{\partial p}{\partial x_1}\right|_{x_1=h/2} = \frac{1}{2}\,\left.\frac{\partial p}{\partial x_1}\right|_{x_1=0} + \frac{1}{2}\,\frac{p_{2j}-p_{1j}}{h} + O(h^2) = \frac{2}{3}\,\frac{p_{1j}-p_{0j}}{h/2} + \frac{1}{3}\,\frac{p_{2j}-p_{1j}}{h} + O(h^2).$$

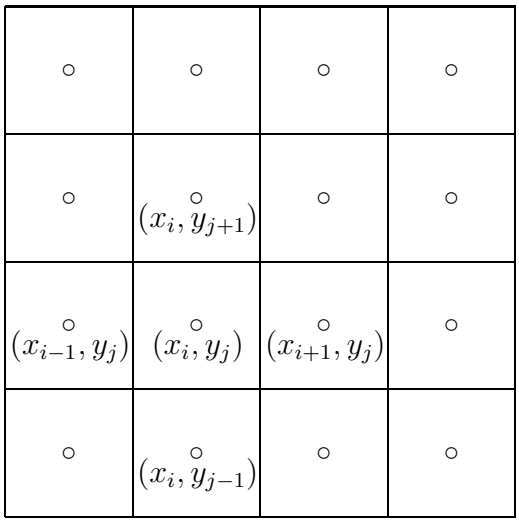

Figure 1: An example of a cell-centered grid with 16 control volumes.

A nonlinear (FAS) multigrid iterative method (to be described below) is used to solve the above system of nonlinear algebraic equations. On each grid, a single grid solver based on the *Picard method* (i.e., the nonlinear coefficients are computed using the previous iterate p) is used. In this case the linearized system looks as follows:

$$\begin{aligned} & h_2 \left[a^{(s-1)}_{i+1/2,j} \frac{p^{(s)}_{i+1,j} - p^{(s)}_{ij}}{h_1} - a^{(s-1)}_{i-1/2,j} \frac{p^{(s)}_{ij} - p^{(s)}_{i-1,j}}{h_1} \right] \quad + \\ & h_1 \left[b^{(s-1)}_{i,j+1/2} \frac{p^{(s)}_{i,j+1} - p^{(s)}_{ij}}{h_2} - b^{(s-1)}_{i,j-1/2} \frac{p^{(s)}_{ij} - p^{(s)}_{i,j-1}}{h_2} \right] \quad = h_1 h_2 f^{(s-1)}_{ij}. \end{aligned} \tag{2}$$

The resulting system of linear algebraic equations is iterated using the symmetric Gauss-Seidel Method (i.e., two Gauss-Seidel sweeps are performed on each linear iteration, in the second sweep the unknowns are updated in the reverse order).

3 Multigrid adaptive local refinement algorithm

A nonlinear *full-multigrid, full-approximation-storage algorithm* (FMG-FAS) [19, 20], which uses the aforementioned single-grid solver as a smoother, has been implemented. The algorithm is briefly described below (see also Fig. 2).
In order to account for the nonlinearity of the problem, the FMG is combined with the FAS algorithm. The consecutive steps of a *two-grid algorithm* are listed below:

- Perform ν_1 *nonlinear pre-relaxations* (i.e., iterate (2) for $s = 1, 2, ..., \nu_1$) on $N^h(u^h) = f^h$ on the fine grid;

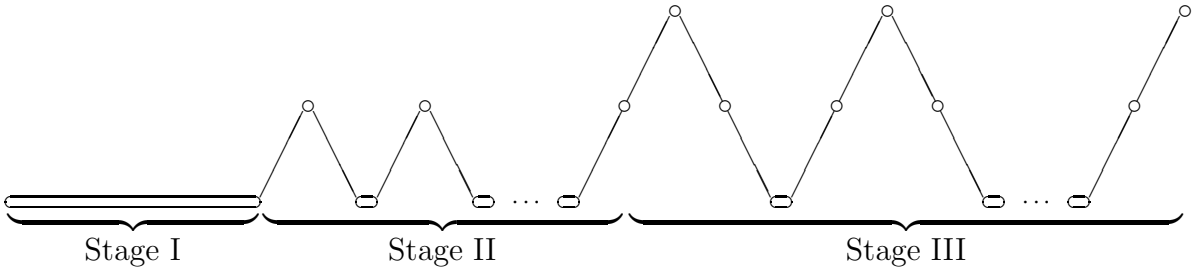

Figure 2: FMG with 3 stages (V-cycles).

- Compute the residual $r^h := f^h - N^h(u^h)$ and transfer it to the coarse grid $r^{2h} := I_h^{2h} r^h$;
- Transfer the fine grid solution to the coarse grid $\bar{u}^{2h} := I_h^{2h} u^h$;
- Solve (exactly, or perform ν_{cg} nonlinear iterations for) the coarse grid equation $N^{2h}(u^{2h}) = r^{2h} + N^{2h}(\bar{u}^{2h})$, in order to obtain the correction $c^{2h} := u^{2h} - \bar{u}^{2h}$;
- Interpolate the correction to the fine grid and correct the fine-grid solution $u^h \leftarrow u^h + I_{2h}^h c^{2h}$;
- Perform ν_2 *nonlinear post-relaxations* on $N^h(u^h) = f^h$ on the fine grid.

The restriction operator for the residuals is obtained by the volumes' weighted summation of the residuals over the underlying fine-grid control volumes (CVs), while the projection of the solution is obtained as a mean value. Bilinear and quadratic prolongation operators are employed.
Let us denote by p^c and p^f the values of p on the coarse and fine grid, respectively. For two-dimensional problems, the fine grid volumes with indices $(2i-1, 2j-1)$, $(2i-1, 2j)$, $(2i, 2j-1)$ and $(2i, 2j)$ will form a coarse grid volume denoted by the index (i, j). Then the bilinear interpolation for the fine grid volume $(2i, 2j)$ is given by

$$p^f_{2i,2j} = \frac{9}{16}p^c_{ij} + \frac{3}{16}p^c_{i,j+1} + \frac{3}{16}p^c_{i+1,j} + \frac{1}{16}p^c_{i+1,j+1},$$

while the quadratic interpolation uses the coarse grid solution in the nearest 6 (10 in 3D) coarse grid volumes

$$p^f_{2i,2j} = \frac{15}{16}p^c_{ij} + \frac{3}{32}p^c_{i,j+1} + \frac{3}{32}p^c_{i+1,j} + \frac{1}{16}p^c_{i+1,j+1} - \frac{3}{32}p^c_{i-1,j} - \frac{3}{32}p^c_{i,j-1}.$$

A local refinement multigrid algorithm on a *composite grid* (see Fig. 3) is used. The algorithm is suggested in [3] for vertex based grids, it is extended in [5, 6] to the case of cell centered grids with nested centers, and is discussed in [21, 22] for the case of cell

centered grids with non-nested centers. Here we do a mass conserving discretization on the composite grid, i.e., the flux over an irregular coarse-grid volume wall is the sum of the fluxes over the corresponding walls at the neighbouring fine-grid irregular volumes. In order to approximate the fluxes at the fine-grid irregular volumes, we introduce additional (auxiliary) points, in which the values of the solution are obtained by bilinear or quadratic interpolation on the coarse grid. We employed quadratic interpolation because the bilinear interpolation does not ensure second order approximation for the fluxes u_1 and u_2 on the interface between coarse and fine grid. The fine grid–smoother works only within the refined subdomain, but on the lower grid levels the additional source term in FAS has to be calculated for the irregular coarse-grid CVs, as well.

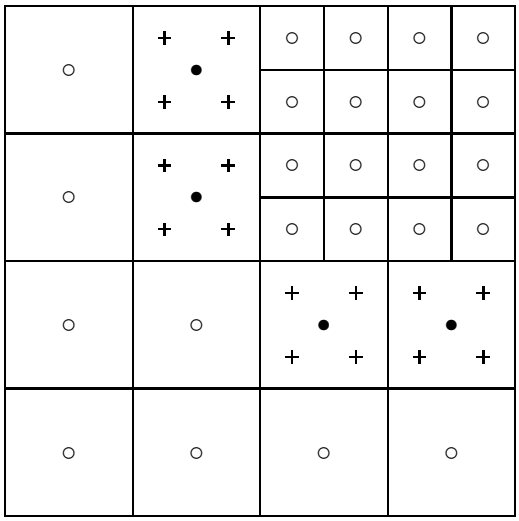

Figure 3: An example of a composite grid, with "•" the centers of the coarse grid irregular CVs are presented, with "+" the auxiliary points are marked.

The software design of the solver is based on the object oriented approach. The latter makes possible to distinguish the different levels of the algorithm not only from a logical, but also from implementational point of view. This advantage is of a general importance, because it facilitates eventual changes in the code: one could modify the algorithm on certain level only, preserving the overall organization of the program. The different levels of the MG-AR algorithm could be clearly distinguished: (i) local discretization within the CV, (ii) global matrix assembly on single grid level, and (iii) multigrid or local refinement algorithm working on inter-grid level. The combination of levels (i) and (ii) is essentially the same as the standard finite element style, because the numerics in both cases is local. Quite naturally, the basic classes in the object oriented

hierarchy correspond with the different levels of the algorithm. The particular advantage is that by designing and implementing a separate CV-class we handle our structured (sets of) meshes in an unstructured way, making possible the refinement within an arbitrary subset of CVs belonging to certain grid level.

Adaptive refinement criterion. Two residual based error indicators are used. The first one [11, 12] is based on a posteriori error estimate for the finite element (FE) method for linear elliptic partial differential equations

Finite element (FE) error indicator.

$$\begin{aligned} g^2(T) &:= \sum_{E\subset\partial T/\partial\Omega} h\frac{1}{\max\limits_{E}|\mathbf{An}|}\left\|\left[(\mathbf{A}\boldsymbol{\nabla}p_h)\cdot\mathbf{n}\right]\right\|^2_{L^2(E)} \\ &+ h^2\frac{1}{\max\limits_{T} a_{\max}}\left\|\boldsymbol{\nabla}\cdot(\mathbf{A}\boldsymbol{\nabla}p_h) - f_h\right\|^2_{L^2(T)}, \end{aligned} \tag{3}$$

where T stands for the current CV, p_h is a bilinear interpolant to the solution defined by its values in the nodes of T (and these values are obtained by bilinear interpolation using the values of the discrete solution in the centers of the CVs), $\mathbf{A}$ is a diagonal matrix with diagonal entries $a_{dd} := k_d\,(\partial p_h/\partial x_d)$, $d = 1, 2$, $a_{\max} := \max(a_{11}, a_{22})$ and $[\,.\,]_E$ denotes the difference between limits from either side of the edge E (with fixed normal direction $\mathbf{n}$). Note, that in our case the term $\boldsymbol{\nabla}\cdot(\mathbf{A}\boldsymbol{\nabla}p_h)$ is identically equal to zero, because we use a bilinear interpolant to the solution in each element.
The second residual based error indicator [13] is based on a posteriori error estimate for the mixed finite element (MFE) method for Raviart-Thomas (RT_0) elements of lowest order

Mixed finite element (MFE) error indicator.

$$g^2(T) := \sum_{E\subset\partial T} h_E\left\|\left[\mathbf{v_h}\cdot\mathbf{t}\right]\right\|^2_{L^2(E)} + h_T^2\left\|\boldsymbol{\nabla}\cdot\mathbf{u_h} - f\right\|^2_{L^2(T)} + h_T^2\left\|\mathbf{v_h}\right\|^2_{L^2(T)}, \tag{4}$$

where $\mathbf{t}$ is a fixed tangential direction to the edge E, $\mathbf{v_h} = (v_{1,h}, v_{2,h}) \in RT_0$ is defined by its values in the centers of the corresponding edges of the CV, i.e., for example $v_{1,h}$ is defined by its values at $(x_{i-1/2}, y_j)$ and $(x_{i+1/2}, y_j)$

$$v_{i-1/2,j} := (p_{ij} - p_{i-1,j})/h_1 \quad \text{and} \quad v_{i+1/2,j} := (p_{i+1,j} - p_{ij})/h_1.$$

Then $\mathbf{u_h} = (u_{1,h}, u_{2,h}) \in RT_0$ and for example $u_{1,h}$ is defined by

$$u_{i-1/2,j} := k_1(v_{i-1/2,j})v_{i-1/2,j} \quad \text{and} \quad u_{i+1/2,j} := k_1(v_{i+1/2,j})v_{i+1/2,j}.$$

Note, there are other ways to define $\mathbf{v_h}$, it is not necessary $\mathbf{v_h} \in RT_0$. In order to compute the jumps of $\mathbf{v_h}$ on the boundary edges, we use the prescribed boundary condition.

Different refinement strategies may be used with these local indicators. Here we use only the *maximum strategy*, i.e., the adaptive refinement at the end of stage l, for some $1 \leq l \leq l_{\max} - 1$, is done for all CVs T of the composite grid Ω_l, satisfying

$$g(T) > \gamma \max_{T' \subset \Omega_l} g(T'). \tag{5}$$

In addition to the set of elements that are marked in this way, we also mark all their neighbors with a common edge (3D: face). We moreover add to this set those elements that now have more than half of the neighbors marked.

4 Numerical experiments

Two sets of numerical experiments are performed. In the first set, the exact solution of the problem is known, and the order of the convergence and the efficiency of the algorithm can be carefully investigated. Namely, the influence of the quadratic interpolation, influence of near-boundary discretization, the choice of the error indicator, the influence of the degree of the nonlinearity, etc. are studied. In the second set, practice induced problems are solved. These are related to liquid polymer moulding process, where a liquid polymer (which is a non Newtonian fluid) flows through a porous preform [23]. Because the exact solution is not known in this case, we compare the solution on the adaptively locally refined grid with a global solution on a very fine grid.

In the first two examples presented below, the boundary conditions (Dirichlet) and the right hand side f correspond to an exact solution of the form:

$$p(x, y; a, b, \xi, \eta, \alpha, \beta) = \exp\Big(-\frac{1}{a^2}(x^2 - \xi^2) - \frac{1}{b^2}(y^2 - \eta^2)\Big) - \alpha x - \beta y,$$

where a, b, ξ, η, α, β are parameters, a and b influence the steepness of the solution and its symmetry, ξ and η determine the location of the maximum of p, α and β may be used to add some additional non-symmetry in the solution and to prevent the problem from degeneration.
In all cases, $\nu_1 = 1$ nonlinear pre-smoothing and $\nu_2 = 2$ nonlinear post-smoothings are performed on the finer grid levels, while on the coarsest grid $\nu_{cg} = 30$ nonlinear smoothings are done. Five symmetric Gauss-Seidel linear iterations are performed within each nonlinear smoothing. The multigrid sweeps on a fixed grid are performed until the algebraic residuals fall 10^{-7} times, followed by a refinement and solving on the refined grid. Six levels of refinement are used and the refinement on the first two grids is always global, i.e., within the whole domain.

Example 1. Some results for the case $K_1 = K_2 = 1,\ a = 0.2,\ b = 0.4,\ \xi = -0.05,\ \eta = -0.10,\ \alpha = \beta = 0.1$ are presented in Tables 1 – 12. In the first column of all tables the

number of the corresponding level of refinement (*stage* 'st') is given, where 1 denotes the coarsest grid with 10×10 control volumes (CVs). The other notations are: *sweeps* 'sw' stands for the number of nonlinear multigrid iterations, $\| e_0 \|_C$, $\| e_1 \|_C$ and $\| e_2 \|_C$ stand for the discrete maximum-norm of the error for the pressure p and the velocities u_1 and u_2 respectively, while $\| e_0 \|_{L_2}$, $\| e_1 \|_{L_2}$ and $\| e_2 \|_{L_2}$ denote the corresponding discrete L^2-norm. An additional notation is the order of convergence α, computed by the formula

$$\alpha = 2\frac{\ln(e_{l-1}) - \ln(e_l)}{\ln(\mathrm{CVs}_l) - \ln(\mathrm{CVs}_{l-1})},$$

where l represents the current stage, $e = e_0, e_1$, or e_2.

Table 1: Multigrid performance, $m = 0$.

st	sw	CVs	$\| e_0 \|_C$	$\| e_1 \|_C$	$\| e_2 \|_C$	$\| e_0 \|_{L_2}$	$\| e_1 \|_{L_2}$	$\| e_2 \|_{L_2}$
without correction of the boundary fluxes								
2	3	400	8.1e-3	1.1e-1	1.2e-1	9.7e-4	8.8e-3	7.1e-3
3	3	1600	2.4e-3	6.0e-2	6.4e-2	2.4e-4	2.4e-3	2.1e-3
4	3	6400	6.5e-4	3.2e-2	3.3e-2	6.1e-5	6.7e-4	5.8e-4
5	3	25600	1.7e-4	1.6e-2	1.6e-2	1.5e-5	1.8e-4	1.6e-4
6	3	102400	4.4e-5	8.2e-3	8.3e-3	3.8e-6	4.8e-5	4.3e-5
α			2.0	1.0	1.0	2.0	1.9	1.9
$m = 0$, with correction of the boundary fluxes								
2	3	400	3.3e-3	2.3e-2	4.9e-2	7.4e-4	3.8e-3	4.9e-3
3	3	1600	9.2e-4	8.4e-3	1.3e-2	2.1e-4	1.0e-3	1.2e-3
4	3	6400	2.4e-4	2.6e-3	3.5e-3	5.6e-5	2.7e-4	3.0e-4
5	3	25600	6.2e-5	7.0e-4	9.3e-4	1.5e-5	7.0e-5	7.7e-5
6	3	102400	1.6e-5	1.8e-4	2.4e-4	3.7e-6	1.8e-5	1.9e-5
α			2.0	2.0	2.0	2.0	2.0	2.0

Multigrid (MG) performance in the case of global refinement is presented in Tables 1 – 3. The number of multigrid sweeps on each multigrid stage is almost constant, which means that the amount of computations is proportional to the number of CVs. On the other hand, the number of the multigrid sweeps is influenced by the degree of nonlinearity of the considered problem (compare the number of sweeps in Tables 1 – 3). Partially, this is due to the simple linearization approach used.

Table 2: Multigrid performance, $m = 0.5$.

st	sw	CVs	$\| e_0 \|_C$	$\| e_1 \|_C$	$\| e_2 \|_C$	$\| e_0 \|_{L_2}$	$\| e_1 \|_{L_2}$	$\| e_2 \|_{L_2}$
without correction of the boundary fluxes, without aver. of the coeff.								
2	8	400	8.8e-3	2.0e-1	2.3e-1	1.2e-3	1.9e-2	1.3e-2
3	8	1600	2.5e-3	1.2e-1	1.2e-1	2.8e-4	5.2e-3	3.8e-3
4	8	6400	6.6e-4	6.4e-2	5.9e-2	7.0e-5	1.4e-3	1.1e-3
5	8	25600	1.7e-4	3.3e-2	3.0e-2	1.8e-5	3.8e-4	2.9e-4
6	8	102400	4.4e-5	1.7e-2	1.5e-2	4.4e-6	1.0e-4	7.9e-5
α			2.0	1.0	1.0	2.0	1.9	1.9
without correction of the boundary fluxes, arithm. aver.								
2	5	400	9.9e-3	2.5e-1	2.8e-1	1.5e-3	3.8e-2	1.8e-2
3	5	1600	2.7e-3	9.4e-2	1.4e-1	3.8e-4	9.2e-3	4.7e-3
4	5	6400	6.9e-4	5.7e-2	6.4e-2	9.7e-5	2.4e-3	1.2e-3
5	5	25600	1.8e-4	3.2e-2	3.1e-2	2.4e-5	6.0e-4	3.3e-4
6	5	102400	4.5e-5	1.6e-2	1.5e-2	6.1e-6	1.6e-4	8.6e-5
α			2.0	1.0	1.0	2.0	1.9	1.9
with correction of the boundary fluxes, without aver. of the coeff.								
2	8	400	4.4e-3	5.3e-2	8.9e-2	9.9e-4	9.4e-3	8.4e-3
3	8	1600	1.2e-3	2.4e-2	2.6e-2	2.9e-4	2.5e-3	2.0e-3
4	8	6400	3.2e-4	7.8e-3	7.4e-3	7.5e-5	6.6e-4	4.8e-4
5	8	25600	8.1e-5	2.2e-3	2.0e-3	1.9e-5	1.7e-4	1.2e-4
6	8	102400	2.0e-5	5.8e-4	5.1e-4	4.8e-6	4.2e-5	3.0e-5
α			2.0	1.9	2.0	2.0	2.0	2.0
with correction of the boundary fluxes, arithm. aver.								
2	5	400	9.4e-3	2.2e-1	1.7e-1	2.3e-3	3.2e-2	1.8e-2
3	5	1600	2.5e-3	6.4e-2	5.3e-2	6.4e-4	7.2e-3	4.2e-3
4	5	6400	6.6e-4	1.8e-2	1.5e-2	1.7e-4	1.7e-3	1.0e-3
5	5	25600	1.7e-4	4.9e-3	3.9e-3	4.3e-5	4.1e-4	2.6e-4
6	5	102400	4.2e-5	1.3e-3	1.0e-3	1.1e-5	1.0e-4	6.5e-5
α			2.0	1.9	2.0	2.0	2.0	2.0

Table 3: Multigrid performance, $m = 1$.

st	sw	CVs	$\| e_0 \|_C$	$\| e_1 \|_C$	$\| e_2 \|_C$	$\| e_0 \|_{L_2}$	$\| e_1 \|_{L_2}$	$\| e_2 \|_{L_2}$
without correction of the boundary fluxes, arithm. aver.								
2	14	400	1.2e-2	9.5e-1	4.7e-1	2.2e-3	1.3e-1	3.2e-2
3	13	1600	2.8e-3	2.3e-1	2.3e-1	5.6e-4	2.9e-2	8.3e-3
4	13	6400	7.2e-4	9.1e-2	1.0e-1	1.4e-4	7.0e-3	2.2e-3
5	13	25600	1.8e-4	5.5e-2	4.9e-2	3.6e-5	1.8e-3	5.6e-4
6	14	102400	4.6e-5	2.9e-2	2.4e-2	9.0e-6	4.5e-4	1.5e-4
α			2.0	0.9	1.0	2.0	2.0	1.9
with correction of the boundary fluxes, arithm. aver.								
2	14	400	1.5e-2	8.8e-1	4.3e-1	3.7e-3	1.2e-1	3.7e-2
3	11	1600	3.9e-3	1.9e-1	1.2e-1	1.0e-3	2.5e-2	8.0e-3
4	11	6400	1.0e-3	5.2e-2	3.3e-2	2.6e-4	6.0e-3	1.9e-3
5	11	25600	2.6e-4	1.4e-2	8.9e-3	6.6e-5	1.5e-3	4.6e-4
6	11	102400	6.4e-5	3.6e-3	2.3e-3	1.7e-5	3.6e-4	1.2e-4
α			2.0	2.0	2.0	2.0	2.0	1.9

The decrease of the maximum- and L^2-norm of the error shows second order of convergence for p in all cases and for u_1 and u_2 in the cases with boundary flux correction. Without boundary flux correction, the maximum-norm of the error for the velocities shows first order of convergence. If no averaging of the coefficients is used for $m = 0.5$, the errors could be smaller (especially with boundary flux correction), but the convergence is slower. In the case $m = 1$ the scheme without averaging of the coefficients is not convergent at all.

In Tables 4 – 6, results from computations with MG-LR (multigrid - local refinement) solver are presented. After completing computations on the two coarsest grids, the grid in the region $[0, X] \times [0, Y]$ is refined. At the end of the next stages, the grids are refined globally. In this way we solve the problem on a sequence of composite grids.

As it can be seen, when quadratic interpolation is used, second order of convergence in maximum- and L^2-norm for p, u_1 and u_2 is obtained. When bilinear prolongation is used, the results show second order convergence in maximum- and L^2-norm for the pressure, second order convergence in L^2-norm for the velocities, but first order convergence in maximum norm for the velocities.

In Tables 7 – 9, MG with adaptive local refinement (AR) is presented for the finite

Table 4: MG performance with LR at the end of the 2nd stage in $[0, X] \times [0, Y]$, $m = 0$.

st	sw	CVs	$\| e_0 \|_C$	α	$\| e_1 \|_C$	α	$\| e_2 \|_C$	α	$\| e_0 \|_{L_2}$	α	$\| e_1 \|_{L_2}$	α	$\| e_2 \|_{L_2}$	α
X=0.3, Y=0.45														
quadratic interpolation														
2	3	400	3.3e-3		2.3e-2		4.9e-2		7.4e-4		3.8e-3		4.9e-3	
3	3	562	7.9e-4	8.4	8.5e-3	5.8	1.3e-2	7.9	1.9e-4	7.9	1.5e-3	5.6	1.3e-3	7.9
4	4	2248	2.2e-4	1.8	2.6e-3	1.7	3.4e-3	1.9	5.6e-5	1.8	3.6e-4	2.0	3.2e-4	2.0
5	4	8992	5.9e-5	1.9	7.0e-4	1.9	9.1e-4	1.9	1.5e-5	1.9	9.1e-5	2.0	8.1e-5	2.0
6	4	35968	1.5e-5	2.0	1.8e-4	2.0	2.4e-4	1.9	3.9e-6	1.9	2.3e-5	2.0	2.1e-5	2.0
bilinear interpolation														
2	3	400	3.3e-3		2.3e-2		4.9e-2		7.4e-4		3.8e-3		4.9e-3	
3	3	562	8.7e-4	7.8	4.2e-2	-3.6	4.1e-2	1.1	1.9e-4	8.0	2.8e-3	1.7	2.1e-3	4.9
4	3	2248	2.7e-4	1.7	2.2e-2	.9	2.2e-2	.9	5.3e-5	1.9	7.4e-4	1.9	5.8e-4	1.9
5	3	8992	7.6e-5	1.8	1.1e-2	1.0	1.1e-2	1.0	1.4e-5	1.9	2.0e-4	1.9	1.6e-4	1.9
6	3	35968	2.0e-5	1.9	5.7e-3	1.0	5.7e-3	1.0	3.5e-6	2.0	5.1e-5	1.9	4.1e-5	1.9
X=0.1, Y=0.15														
quadratic interpolation														
2	3	400	3.3e-3		2.3e-2		4.9e-2		7.4e-4		3.8e-3		4.9e-3	
3	4	418	2.9e-3	5.1	2.7e-2	-8.5	4.2e-2	7.4	6.5e-4	5.7	3.7e-3	.3	4.0e-3	9.0
4	5	1672	8.3e-4	1.8	7.0e-3	2.0	1.1e-2	1.9	1.9e-4	1.8	8.6e-4	2.1	1.0e-3	2.0
5	5	6688	2.2e-4	1.9	1.8e-3	2.0	3.0e-3	1.9	5.1e-5	1.9	2.1e-4	2.0	2.6e-4	2.0
6	5	26752	5.6e-5	2.0	4.4e-4	2.0	8.0e-4	1.9	1.3e-5	2.0	5.4e-5	2.0	6.6e-5	2.0
bilinear interpolation														
2	3	400	3.3e-3		2.3e-2		4.9e-2		7.4e-4		3.8e-3		4.9e-3	
3	2	418	3.2e-3	1.6	4.1e-2	-26.6	4.1e-2	7.7	7.1e-4	1.9	3.8e-3	.0	4.7e-3	2.1
4	3	1672	8.5e-4	1.9	3.0e-2	.5	2.8e-2	.6	2.0e-4	1.8	1.1e-3	1.7	1.4e-3	1.8
5	3	6688	2.2e-4	1.9	1.7e-3	.8	1.6e-2	.8	5.2e-5	1.9	3.3e-4	1.8	3.8e-4	1.8
6	3	26752	5.6e-5	2.0	9.3e-3	.9	8.7e-3	.9	1.3e-5	2.0	9.1e-5	1.8	1.0e-4	1.9

Table 5: MG performance with LR at the end of the 2nd stage in $[0, X] \times [0, Y]$, $m = 0.5$.

st	sw	CVs	$\| e_0 \|_C$	α	$\| e_1 \|_C$	α	$\| e_2 \|_C$	α	$\| e_0 \|_{L_2}$	α	$\| e_1 \|_{L_2}$	α	$\| e_2 \|_{L_2}$	α
X=0.3, Y=0.45														
quadratic interpolation														
2	5	400	9.4e-3		2.2e-1		1.7e-1		2.3e-3		3.2e-2		1.8e-2	
3	5	562	2.4e-3	8.1	6.4e-2	7.4	5.1e-2	7.2	5.9e-4	8.0	7.5e-3	8.5	4.0e-3	8.8
4	6	2248	6.2e-4	1.9	1.8e-2	1.8	1.4e-2	1.8	1.6e-4	1.9	1.8e-3	2.1	9.8e-4	2.0
5	6	8992	1.6e-4	2.0	4.9e-3	1.9	3.8e-3	1.9	4.1e-5	2.0	4.4e-4	2.0	2.5e-4	2.0
6	6	35968	4.0e-5	2.0	1.3e-3	1.9	9.9e-4	1.9	1.0e-5	2.0	1.1e-4	2.0	6.3e-5	2.0
bilinear interpolation														
2	5	400	9.4e-3		2.2e-1		1.7e-1		2.3e-3		3.2e-2		1.8e-2	
3	5	562	2.2e-3	8.6	6.5e-2	7.3	4.8e-2	7.5	5.8e-4	8.1	8.6e-3	7.8	4.2e-3	8.4
4	5	2248	5.7e-4	1.9	2.9e-2	1.2	1.5e-2	1.6	1.6e-4	1.9	2.0e-3	2.1	1.1e-3	2.0
5	5	8992	1.5e-4	2.0	1.4e-2	1.0	8.1e-3	.9	4.0e-5	2.0	5.1e-4	2.0	2.7e-4	2.0
6	5	35968	3.7e-5	2.0	7.0e-3	1.0	4.2e-3	.9	1.0e-5	2.0	1.3e-4	2.0	6.8e-5	2.0
X=0.1, Y=0.15														
quadratic interpolation														
2	5	400	9.4e-3		2.2e-1		1.7e-1		2.3e-3		3.2e-2		1.8e-2	
3	8	418	7.8e-3	8.2	1.4e-1	23.1	1.3e-1	13.3	1.9e-3	8.6	2.4e-2	14.0	1.2e-2	17.5
4	8	1672	2.1e-3	1.9	3.8e-2	1.8	3.6e-2	1.8	5.4e-4	1.8	5.7e-3	2.1	3.0e-3	2.0
5	8	6688	5.5e-4	1.9	1.1e-2	1.8	1.0e-2	1.8	1.4e-4	1.9	1.4e-3	2.0	7.5e-4	2.0
6	8	26752	1.4e-4	2.0	3.1e-3	1.8	2.8e-3	1.9	3.6e-5	2.0	3.5e-4	2.0	1.9e-4	2.0
bilinear interpolation														
2	5	400	9.4e-3		2.2e-1		1.7e-1		2.3e-3		3.2e-2		1.8e-2	
3	5	418	8.1e-3	6.6	1.8e-1	9.2	1.3e-1	11.9	2.0e-3	6.7	2.4e-2	13.5	1.3e-2	15.5
4	5	1672	2.2e-3	1.9	7.2e-2	1.4	5.7e-2	1.2	5.5e-4	1.9	5.9e-3	2.0	3.6e-3	1.8
5	5	6688	5.5e-4	2.0	3.3e-2	1.1	3.5e-2	.7	1.4e-4	1.9	1.5e-3	2.0	9.9e-4	1.9
6	5	26752	1.4e-4	2.0	1.7e-2	.9	1.9e-2	.9	3.6e-5	2.0	3.8e-4	2.0	2.7e-4	1.9

Table 6: MG performance with LR at the end of the 2nd stage in $[0, X] \times [0, Y]$, $m = 1$.

st	sw	CVs	$\| e_0 \|_C$	α	$\| e_1 \|_C$	α	$\| e_2 \|_C$	α	$\| e_0 \|_{L_2}$	α	$\| e_1 \|_{L_2}$	α	$\| e_2 \|_{L_2}$	α
X=0.3, Y=0.45														
quadratic interpolation														
2	14	400	1.5e-2		8.8e-1		4.3e-1		3.7e-3		1.2e-1		3.7e-2	
3	13	562	3.7e-3	8.2	2.0e-1	8.8	1.2e-1	7.6	9.1e-4	8.2	2.5e-2	9.2	7.6e-3	9.3
4	14	2248	9.5e-4	2.0	5.3e-2	1.9	3.2e-2	1.8	2.4e-4	1.9	5.9e-3	2.1	1.8e-3	2.1
5	15	8992	2.4e-4	2.0	1.4e-2	1.9	8.7e-3	1.9	6.0e-5	2.0	1.5e-3	2.0	4.4e-4	2.0
6	15	35968	6.0e-5	2.0	3.6e-3	2.0	2.3e-3	1.9	1.5e-5	2.0	3.6e-4	2.0	1.1e-4	2.0
bilinear interpolation														
2	14	400	1.5e-2		8.8e-1		4.3e-1		3.7e-3		1.2e-1		3.7e-2	
3	11	562	3.6e-3	8.4	2.0e-1	8.8	1.1e-1	7.8	9.0e-4	8.2	2.5e-2	9.1	7.7e-3	9.3
4	11	2248	9.3e-4	2.0	5.3e-2	1.9	3.2e-2	1.8	2.4e-4	1.9	6.0e-3	2.1	1.8e-3	2.1
5	11	8992	2.3e-4	2.0	1.4e-2	1.9	8.6e-3	1.9	6.0e-5	2.0	1.5e-3	2.0	4.5e-4	2.0
6	11	35968	5.9e-5	2.0	6.9e-3	1.0	4.3e-3	1.0	1.5e-5	2.0	3.7e-4	2.0	1.1e-4	2.0
X=0.1, Y=0.15														
quadratic interpolation														
2	14	400	1.5e-2		8.8e-1		4.3e-1		3.7e-3		1.2e-1		3.7e-2	
3	13	418	1.2e-2	10.3	4.4e-1	31.1	2.9e-1	17.8	2.9e-3	10.9	7.8e-2	18.9	2.4e-2	20.8
4	14	1672	3.1e-3	1.9	1.5e-1	1.6	7.3e-2	2.0	8.0e-4	1.9	1.9e-2	2.0	5.2e-3	2.2
5	15	6688	8.0e-4	2.0	4.8e-2	1.6	2.1e-2	1.8	2.1e-4	1.9	4.7e-3	2.0	1.3e-3	2.0
6	15	26752	2.0e-4	2.0	1.3e-2	1.8	5.9e-3	1.8	5.3e-5	2.0	1.2e-3	2.0	3.1e-4	2.0
bilinear interpolation														
2	14	400	1.5e-2		8.8e-1		4.3e-1		3.7e-3		1.2e-1		3.7e-2	
3	11	418	1.2e-2	9.3	5.4e-1	21.7	2.7e-1	21.4	3.0e-3	9.2	7.7e-2	19.5	2.4e-2	21.1
4	11	1672	3.1e-3	2.0	1.6e-1	1.7	1.1e-1	1.3	8.1e-4	1.9	1.9e-2	2.0	6.3e-3	1.9
5	11	6688	8.0e-4	2.0	6.9e-2	1.2	6.9e-2	.7	2.1e-4	2.0	4.7e-3	2.0	1.8e-3	1.8
6	11	26752	2.0e-4	2.0	3.2e-2	1.1	3.7e-2	.9	5.3e-5	2.0	1.2e-3	2.0	5.0e-4	1.8

Table 7: MG–AR performance, FE error indicator, $m = 0$.

st	sw	CVs	$\| e_0 \|_C$	$\| e_1 \|_C$	$\| e_2 \|_C$	$\| e_0 \|_{L_2}$	$\| e_1 \|_{L_2}$	$\| e_2 \|_{L_2}$
$\gamma = 0.2$								
2	3	400	3.3e-3	2.3e-2	4.9e-2	7.4e-4	3.8e-3	4.9e-3
3	5	598	8.7e-4	8.4e-3	1.3e-2	2.0e-4	1.2e-3	1.2e-3
4	5	1360	2.2e-4	2.6e-3	3.6e-3	6.8e-5	4.6e-4	3.8e-4
5	5	3961	8.3e-5	1.1e-3	2.0e-3	3.3e-5	1.9e-4	1.5e-4
6	5	13282	3.7e-5	5.4e-4	7.4e-4	1.5e-5	7.3e-5	6.2e-5
$\gamma = 0.1$								
2	3	400	3.3e-3	2.3e-2	4.9e-2	7.4e-4	3.8e-3	4.9e-3
3	4	676	8.9e-4	8.4e-3	1.3e-2	1.9e-4	1.1e-3	1.2e-3
4	4	1720	2.2e-4	2.6e-3	3.4e-3	5.5e-5	3.4e-4	3.2e-4
5	4	5539	5.3e-5	7.0e-4	8.8e-4	2.2e-5	1.2e-4	1.0e-4
6	4	19441	2.3e-5	3.0e-4	5.5e-4	9.6e-6	4.5e-5	3.8e-5
$\gamma = 0.05$								
2	3	400	3.3e-3	2.3e-2	4.9e-2	7.4e-4	3.8e-3	4.9e-3
3	4	751	9.1e-4	8.4e-3	1.3e-2	2.0e-4	1.1e-3	1.2e-3
4	4	2065	2.3e-4	2.6e-3	3.5e-3	5.1e-5	2.9e-4	3.0e-4
5	4	6931	5.6e-5	7.0e-4	9.0e-4	1.6e-5	9.1e-5	8.4e-5
6	4	25519	1.4e-5	1.8e-4	2.3e-4	5.9e-6	2.9e-5	2.6e-5
$\gamma = 0.05$, bilinear prolongation in auxiliary								
2	3	400	3.3e-3	2.3e-2	4.9e-2	7.4e-4	3.8e-3	4.9e-3
3	3	751	9.0e-4	8.4e-3	1.3e-2	1.9e-4	1.0e-3	1.2e-3
4	3	2065	2.2e-4	2.6e-3	3.4e-3	4.6e-5	3.1e-4	3.2e-4
5	3	6940	5.3e-5	1.4e-3	1.6e-3	1.7e-5	1.0e-4	8.8e-5
6	3	25519	1.2e-5	8.6e-4	9.6e-4	4.7e-6	3.5e-5	2.7e-5

Table 8: MG–AR performance, FE error indicator, $m = 0.5$.

st	sw	CVs	$\| e_0 \|_C$	$\| e_1 \|_C$	$\| e_2 \|_C$	$\| e_0 \|_{L_2}$	$\| e_1 \|_{L_2}$	$\| e_2 \|_{L_2}$
$\gamma = 0.1$								
2	5	400	9.4e-3	2.2e-1	1.7e-1	2.3e-3	3.2e-2	1.8e-2
3	9	634	2.5e-3	6.4e-2	5.2e-2	6.0e-4	7.2e-3	4.1e-3
4	6	1504	6.4e-4	1.8e-2	1.4e-2	1.5e-4	1.7e-3	1.3e-3
5	6	4624	1.6e-4	4.9e-3	3.8e-3	5.0e-5	4.5e-4	2.6e-4
6	7	16159	4.5e-5	2.4e-3	1.4e-3	2.0e-5	1.6e-4	7.4e-5
$\gamma = 0.05$								
2	5	400	9.4e-3	2.2e-1	1.7e-1	2.3e-3	3.2e-2	1.8e-2
3	7	697	2.5e-3	6.4e-2	5.3e-2	6.2e-4	7.2e-3	4.1e-3
4	6	1798	6.5e-4	1.8e-2	1.4e-2	1.5e-4	1.7e-3	1.0e-3
5	6	5848	1.6e-4	4.9e-3	3.8e-3	4.0e-5	4.1e-4	2.6e-4
6	5	21505	4.0e-5	1.3e-3	9.9e-4	1.3e-5	1.0e-4	6.5e-5

Table 9: MG–AR performance, FE error indicator, $m = 1$.

st	sw	CVs	$\| e_0 \|_C$	$\| e_1 \|_C$	$\| e_2 \|_C$	$\| e_0 \|_{L_2}$	$\| e_1 \|_{L_2}$	$\| e_2 \|_{L_2}$
$\gamma = 0.1$								
2	14	400	1.5e-2	8.8e-1	4.3e-1	3.7e-3	1.2e-1	3.7e-2
3	12	595	3.9e-3	1.9e-1	1.2e-1	9.6e-4	2.5e-2	7.9e-3
4	13	1339	9.8e-4	5.3e-2	3.3e-2	2.5e-4	5.9e-3	1.9e-3
5	12	3964	2.4e-4	1.4e-2	8.8e-3	9.3e-5	1.5e-3	4.7e-4
6	12	13834	9.9e-5	8.3e-3	2.9e-3	4.0e-5	4.9e-4	1.3e-4
$\gamma = 0.05$								
2	14	400	1.5e-2	8.8e-1	4.3e-1	3.7e-3	1.2e-1	3.7e-2
3	14	649	3.9e-3	1.9e-1	1.2e-1	9.4e-4	2.5e-2	8.0e-3
4	12	1585	1.0e-3	5.3e-2	3.3e-2	2.3e-4	5.9e-3	1.9e-3
5	11	5014	2.5e-4	1.4e-2	8.8e-3	6.9e-5	1.4e-3	4.6e-4
6	11	18325	6.2e-5	3.6e-3	2.3e-3	2.5e-5	3.5e-4	1.2e-4

Table 10: MG–AR performance, MFE error indicator, $m = 0$.

st	sw	CVs	$\| e_0 \|_C$	$\| e_1 \|_C$	$\| e_2 \|_C$	$\| e_0 \|_{L_2}$	$\| e_1 \|_{L_2}$	$\| e_2 \|_{L_2}$
$\gamma = 0.2$								
2	3	400	3.3e-3	2.3e-2	4.9e-2	7.4e-4	3.8e-3	4.9e-3
3	4	640	8.4e-4	8.4e-3	1.3e-2	1.8e-4	1.2e-3	1.2e-3
4	5	1606	2.0e-4	2.6e-3	3.4e-3	7.2e-5	4.3e-4	3.9e-4
5	5	5305	8.5e-5	1.0e-3	1.6e-3	3.6e-5	1.7e-4	1.6e-4
6	5	19696	4.2e-5	5.1e-4	6.4e-4	1.6e-5	6.4e-5	6.4e-5
$\gamma = 0.1$								
2	3	400	3.3e-3	2.3e-2	4.9e-2	7.4e-4	3.8e-3	4.9e-3
3	4	706	8.8e-4	8.4e-3	1.3e-2	1.9e-4	1.1e-3	1.2e-3
4	4	1906	2.2e-4	2.6e-3	3.4e-3	5.5e-5	3.4e-4	3.2e-4
5	4	6511	5.4e-5	7.0e-4	9.1e-4	2.2e-5	1.2e-4	1.1e-4
6	5	24520	2.5e-5	3.1e-4	3.5e-4	9.5e-6	4.2e-5	4.1e-5
$\gamma = 0.05$								
2	3	400	3.3e-3	2.3e-2	4.9e-2	7.4e-4	3.8e-3	4.9e-3
3	4	766	9.0e-4	8.4e-3	1.3e-2	2.0e-4	1.0e-3	1.2e-3
4	4	2197	2.3e-4	2.6e-3	3.5e-3	5.1e-5	3.0e-4	3.0e-4
5	4	7699	5.6e-5	7.0e-4	9.0e-4	1.5e-5	9.1e-5	8.4e-5
6	4	29215	1.4e-5	1.8e-4	2.3e-4	5.6e-6	2.9e-5	2.7e-5
$\gamma = 0.05$, bilinear prolongation in auxiliary								
2	3	400	3.3e-3	2.3e-2	4.9e-2	7.4e-4	3.8e-3	4.9e-3
3	3	766	8.9e-4	8.4e-3	1.3e-2	1.9e-4	1.1e-3	1.2e-3
4	3	2203	2.2e-4	5.1e-3	5.8e-3	4.5e-5	3.5e-4	3.1e-4
5	3	7708	5.2e-5	2.7e-3	3.0e-3	1.3e-5	1.1e-4	8.7e-5
6	3	29218	1.3e-5	2.0e-3	2.0e-3	4.6e-6	4.0e-5	3.2e-5

Table 11: MG–AR performance, MFE error indicator, $m = 0.5$.

st	sw	CVs	$\| e_0 \|_C$	$\| e_1 \|_C$	$\| e_2 \|_C$	$\| e_0 \|_{L_2}$	$\| e_1 \|_{L_2}$	$\| e_2 \|_{L_2}$
$\gamma = 0.2$								
2	5	400	9.4e-3	2.2e-1	1.7e-1	2.3e-3	3.2e-2	1.8e-2
3	7	628	2.4e-3	6.4e-2	5.2e-2	5.5e-4	7.2e-3	4.0e-3
4	6	1597	6.2e-4	1.8e-2	1.4e-2	1.5e-4	1.7e-3	1.0e-3
5	7	5287	1.5e-4	4.9e-3	3.7e-3	5.4e-5	4.4e-4	2.6e-4
6	8	19672	5.5e-5	1.4e-3	9.7e-4	2.1e-5	1.2e-4	7.4e-5
$\gamma = 0.1$								
2	5	400	9.4e-3	2.2e-1	1.7e-1	2.3e-3	3.2e-2	1.8e-2
3	6	688	2.5e-3	6.4e-2	5.2e-2	6.0e-4	7.2e-3	4.1e-3
4	6	1900	6.4e-4	1.8e-2	1.4e-2	1.5e-4	1.7e-3	1.0e-3
5	6	6496	1.6e-4	4.9e-3	3.8e-3	4.0e-5	4.1e-4	2.6e-4
6	7	24490	4.0e-5	1.3e-3	9.9e-4	1.3e-5	1.0e-4	6.6e-5

Table 12: MG–AR performance, MFE error indicator, $m = 1$.

st	sw	CVs	$\| e_0 \|_C$	$\| e_1 \|_C$	$\| e_2 \|_C$	$\| e_0 \|_{L_2}$	$\| e_1 \|_{L_2}$	$\| e_2 \|_{L_2}$
$\gamma = 0.2$								
2	14	400	1.5e-2	8.8e-1	4.3e-1	3.7e-3	1.2e-1	3.7e-2
3	14	556	3.6e-3	2.0e-1	1.2e-1	8.5e-4	2.5e-2	7.7e-3
4	15	1348	9.2e-4	5.3e-2	3.2e-2	2.5e-4	5.8e-3	1.8e-3
5	11	4312	3.5e-4	1.4e-2	8.4e-3	1.0e-4	1.5e-3	4.4e-4
6	13	15625	1.3e-4	3.7e-3	2.2e-3	4.2e-5	3.8e-4	1.1e-4
$\gamma = 0.1$								
2	14	400	1.5e-2	8.8e-1	4.3e-1	3.7e-3	1.2e-1	3.7e-2
3	11	619	3.9e-3	1.9e-1	1.2e-1	8.8e-4	2.5e-2	7.9e-3
4	14	1660	9.9e-4	5.3e-2	3.3e-2	2.3e-4	5.9e-3	1.9e-3
5	11	5887	2.5e-4	1.4e-2	8.8e-3	6.0e-5	1.4e-3	4.6e-4
6	11	22333	6.2e-5	3.6e-3	2.3e-3	1.7e-5	3.6e-4	1.1e-4

element error indicator (3) using different values of the parameter γ (see Eq. (5)). In most of the cases (if not denoted explicitly) quadratic prolongation is used. We see that MG-AR solutions for $\gamma = 0.05$ have in maximum norm the same accuracy as those from MG, but significantly less resources (memory, i.e., active CVs, and CPU time) are used in this case. The best choice of γ is still an open question. If too few CVs are selected for refinement (e.g., $\gamma = 0.1$), the accuracy on the composite grid cannot be as good as for $\gamma = 0.05$. Moreover, the number of multigrid sweeps may be greater for MG-AR, if γ is too large. If bilinear prolongation is used in the auxiliary volumes, the convergence in the maximum norm for the velocities is worse in comparison with the case of quadratic prolongation used.

In Tables 10 – 12, MG with adaptive local refinement (AR) is presented for the mixed finite element error indicator (4). The conclusions about the performance of the MG-AR algorithm in this case are similar to those formulated for the FE error indicator. If γ is small enough ($\gamma = 0.05$ for $m = 0$, $\gamma = 0.1$ for $m = 0.5$ and $m = 1$), the MG-AR solutions have the same accuracy in maximum norm as those from MG, but significantly less resources are used.

The dependence of the number of MG sweeps on the number of CVs used in MG and MG-AR solution for $m = 0.5$ is shown on Fig. 4. By MG-AR-FE the MG-AR using the FE error indicator is denoted, while MG-AR-MFE corresponds to MG-AR with MFE error indicator. It is seen that the number of MG sweeps is larger for MG-AR, but this is compensated by the much larger decrease in the number of CVs, used in the computations.

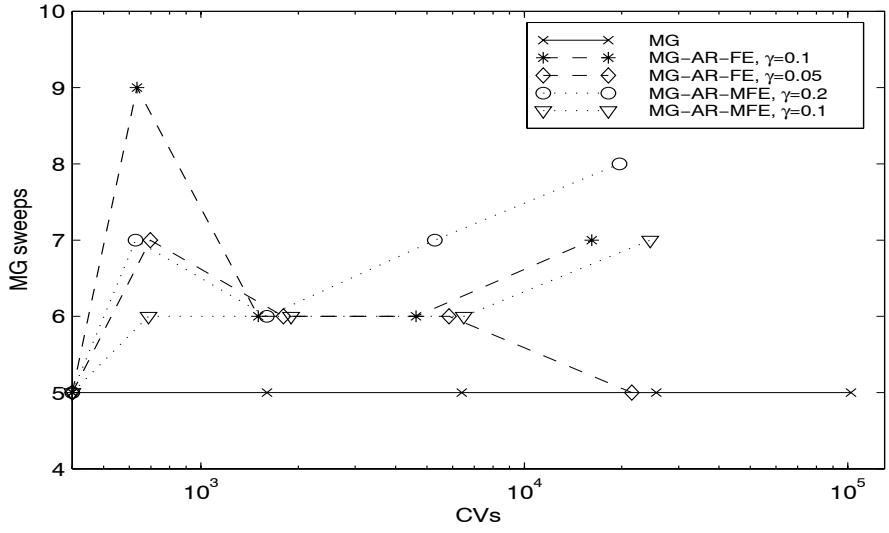

Figure 4: Dependence of the number of MG sweeps on the number of CVs for MG and MG-AR, using FE and MFE error indicators, $m = 0.5$.

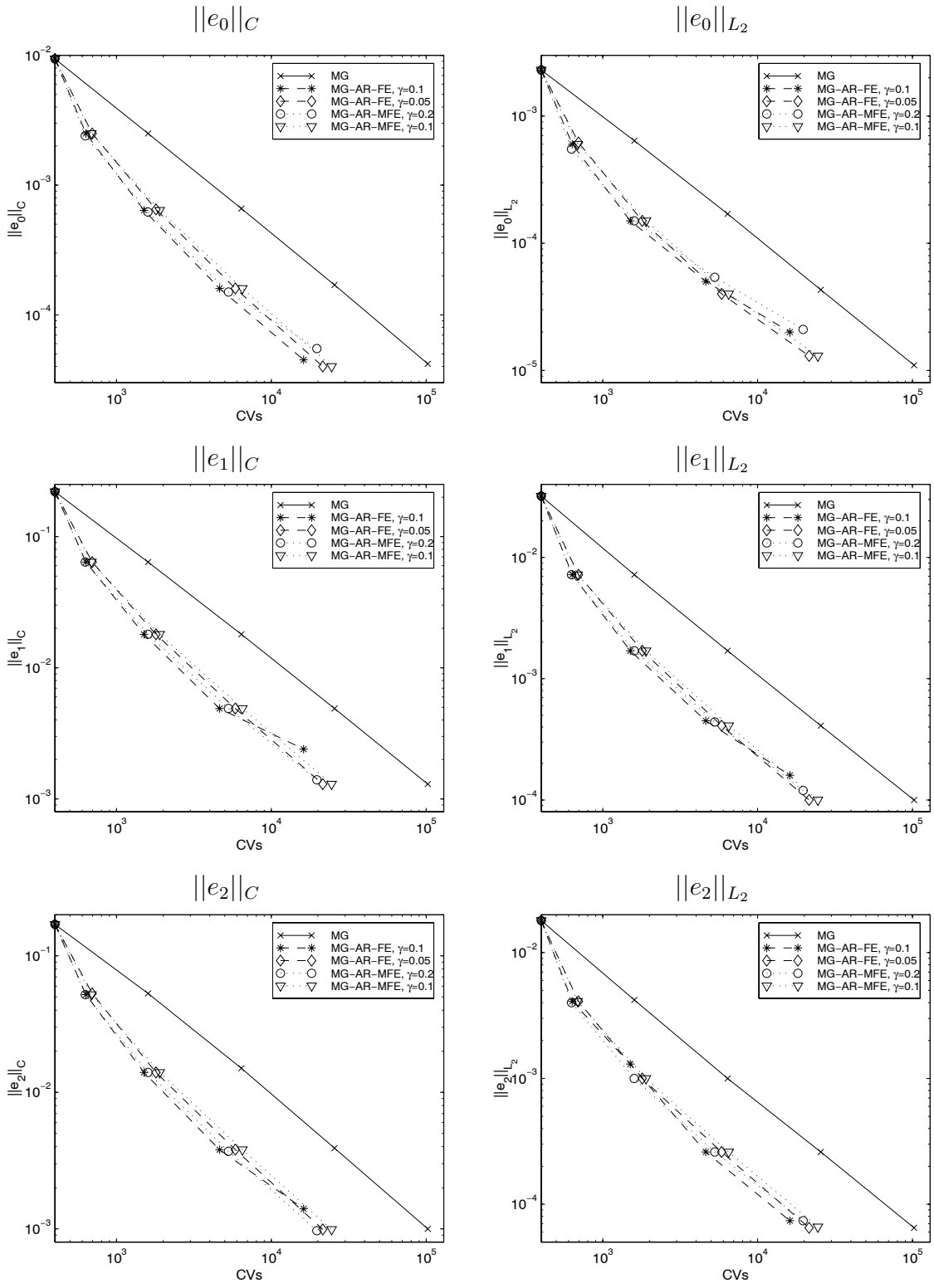

Figure 5: Dependence of the solution accuracy on the number of CVs for MG and MG-AR, using FE and MFE error indicators, $m = 0.5$.

The dependence of the solution accuracy on the number of CVs for MG and MG-AR for $m = 0.5$ is shown on Fig. 5. The left column corresponds to the maximum norm of the error for p, u_1 and u_2 (the first, second and the third row, correspondingly), the right one – to the L_2 norm of the same errors. It is easy to see that the solution accuracy for the smaller values of γ is the same, as for the MG solution, although much less CVs are used in the computations.
The final composite grids for the MG-AR algorithm are shown on Fig. 6 – 8. The figures in the left columns correspond to the FE error indicator, while the figures from the right column correspond to the MFE error indicator. One observes that in both cases the grid is refined in the region where the solution changes rapidly, although there are some differences in the shape of refined domain, depending on the error indicator used.

Example 2. Results for the case $K_1 = K_2 = 1$, $a = b = 0.15$, $\xi = 0.1$, $\eta = 0.3$, $\alpha = \beta = 0$ are presented in Tables 13 – 19. In this case, the maximum of the solution is placed within the computational domain (in $x = \xi$, $y = \eta$) and in the nonlinear case the order of convergence may be not two (as for $m = 0.5$ in Table 13). This is due to the "bad" approximation of the coefficients k_1 and k_2 along the lines $x = 0.1$ and $y = 0.3$ respectively, that is, due to the degeneration of the equation (1) along these lines.
The results about the multigrid performance, presented in Table 13, show that if the nonlinearity is not very strong (e.g. $m = 0.5$), the number of multigrid sweeps on each multigrid stage is almost constant, but for $m = 1$ the number of multigrid sweeps increases with the multigrid stage. As in the previous example, the number of multigrid sweeps is also influenced by the degree of nonlinearity of the problem.
In Tables 14 – 19, MG with adaptive refinement is presented for the finite element error indicator (3) and for the mixed finite element error indicator (4). The MG-AR solutions for the smallest choices of γ have almost the same accuracy in maximum norm, as those obtained with MG, but less resources are used in comparison to MG. The dependence of the number of MG sweeps on the number of CVs used in MG and MG-AR solution for $m = 0.5$ is shown in Fig. 9. The number of multigrid sweeps in all cases is usually larger for MG-AR, but this is compensated by the significant decrease of active CVs, i.e., by much cheaper multigrid iterations.
The dependence of the solution accuracy on the number of CVs for MG and MG-AR for $m = 0.5$ is shown on Fig. 10. It is seen that the solution accuracy for the smaller values of γ is almost the same, as for the MG solution, although much less CVs are used in the computations.
The final composite grids for the MG-AR algorithm are shown on Fig. 11 – 13. The left columns correspond to the FE error indicator, the right ones correspond to the MFE error indicator. In both cases the grid is refined in the region where the solution changes rapidly, although the shape of refined domain depends on the error indicator used, as

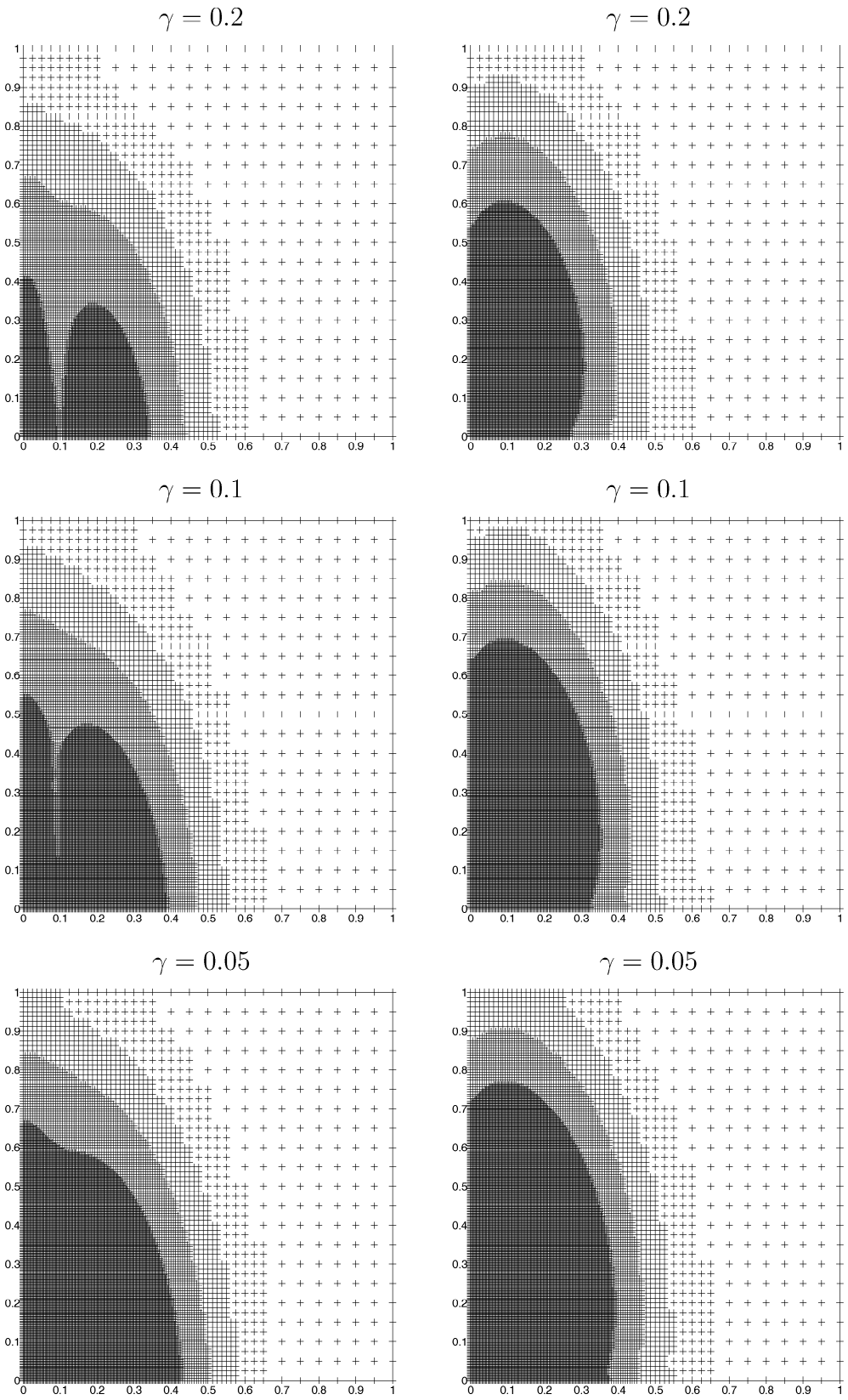

Figure 6: Final composite grids, left – using FE error indicator, right – using MFE error indicator, $m = 0$.

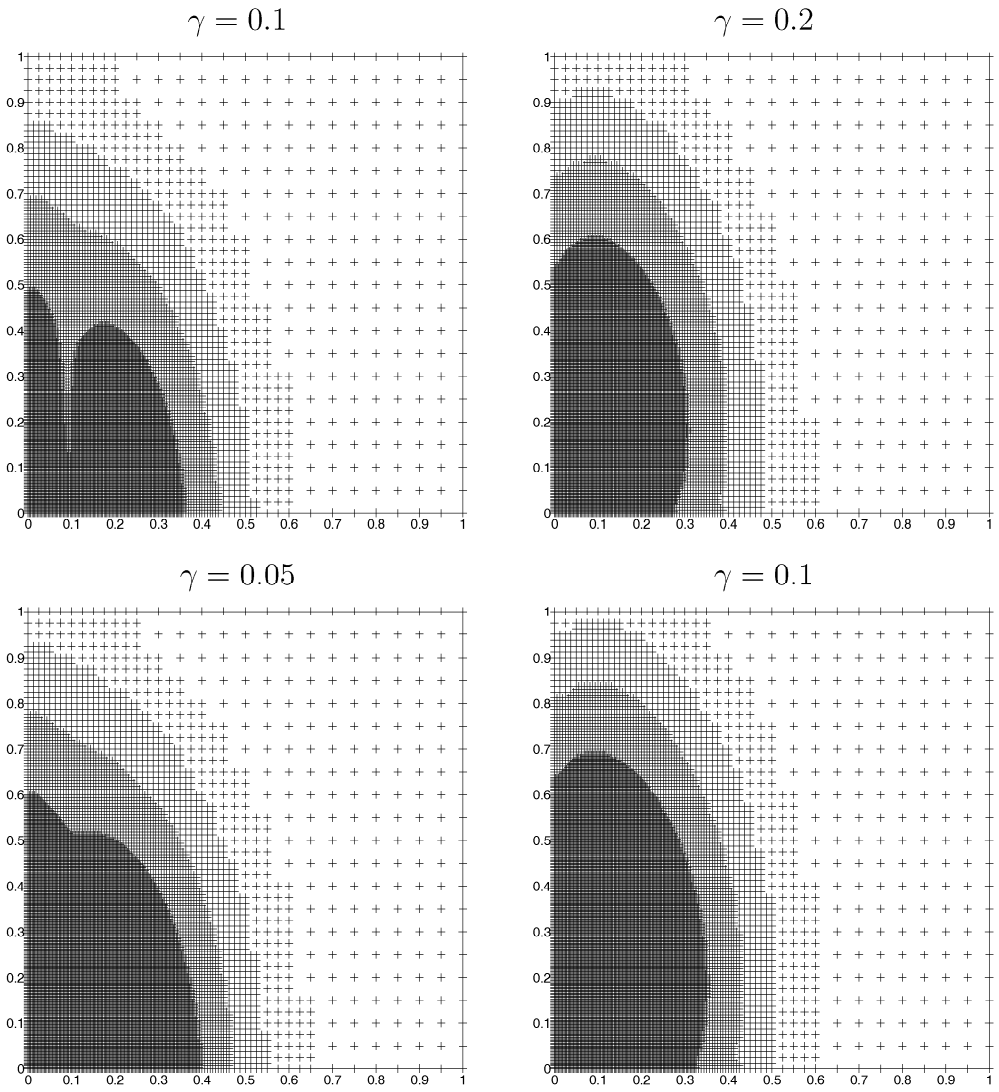

Figure 7: Final composite grids, left – using FE error indicator, right – using MFE error indicator, $m = 0.5$.

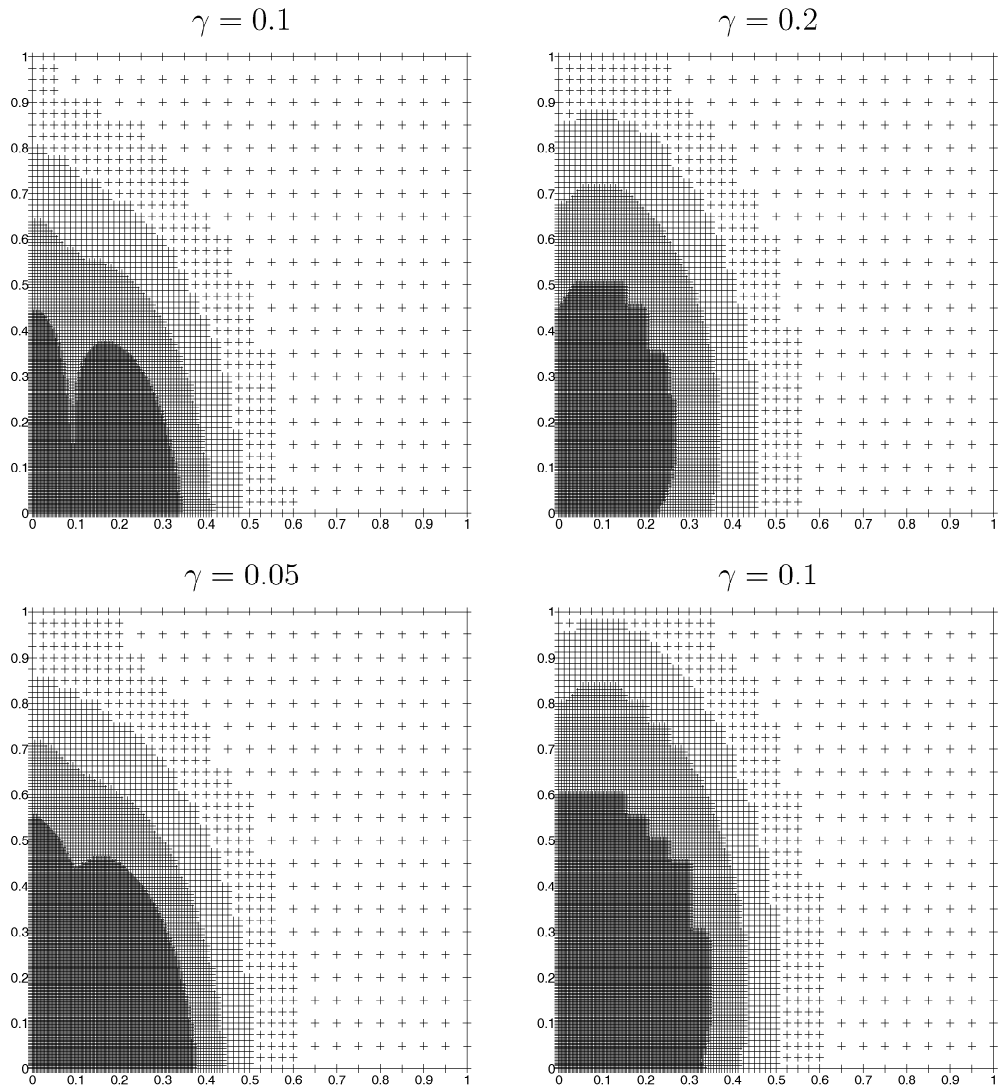

Figure 8: Final composite grids, left – using FE error indicator, right – using MFE error indicator, $m = 1$.

Table 13: Multigrid performance.

st	sw	CVs	$\| e_0 \|_C$	$\| e_1 \|_C$	$\| e_2 \|_C$	$\| e_0 \|_{L_2}$	$\| e_1 \|_{L_2}$	$\| e_2 \|_{L_2}$
$m = 0$								
2	3	400	2.0e-2	2.7e-1	8.6e-2	2.8e-3	2.9e-2	1.6e-2
3	3	1600	5.7e-3	7.1e-2	2.4e-2	7.3e-4	6.5e-3	4.0e-3
4	3	6400	1.5e-3	1.8e-2	6.4e-3	1.9e-4	1.6e-3	1.0e-3
5	3	25600	3.9e-4	4.4e-3	1.6e-3	4.8e-5	3.8e-4	2.6e-4
6	3	102400	9.8e-5	1.1e-3	4.1e-4	1.2e-5	9.5e-5	6.6e-5
α			2.0	2.0	2.0	2.0	2.0	2.0
$m = 0.5$								
2	5	400	1.2e-1	3.6e+0	1.9e+0	2.4e-2	4.2e-1	2.9e-1
3	5	1600	4.0e-2	1.3e+0	5.9e-1	9.8e-3	1.3e-1	8.8e-2
4	6	6400	1.4e-2	4.6e-1	1.9e-1	3.9e-3	4.0e-2	2.8e-2
5	5	25600	4.8e-3	1.7e-1	5.9e-2	1.5e-3	1.3e-2	9.1e-3
6	6	102400	1.7e-3	6.7e-2	2.0e-2	5.8e-4	4.5e-3	3.0e-3
α			1.5	1.3	1.6	1.4	1.5	1.6
$m = 1$								
2	17	400	1.2e-1	8.4e+0	5.9e+0	2.7e-2	1.0e+0	8.4e-1
3	20	1600	3.3e-2	2.5e+0	1.7e+0	9.4e-3	2.5e-1	2.0e-1
4	21	6400	9.0e-3	7.2e-1	4.3e-1	3.0e-3	6.2e-2	4.9e-2
5	24	25600	2.5e-3	1.9e-1	1.1e-1	9.0e-4	1.6e-2	1.2e-2
6	27	102400	6.7e-4	4.7e-2	2.7e-2	2.6e-4	3.9e-3	3.1e-3
α			1.9	2.0	2.0	1.8	2.0	2.0

Table 14: MG-AR performance, FE error indicator, $m = 0$.

st	sw	CVs	$\| e_0 \|_C$	$\| e_1 \|_C$	$\| e_2 \|_C$	$\| e_0 \|_{L_2}$	$\| e_1 \|_{L_2}$	$\| e_2 \|_{L_2}$
$\gamma = 0.1$								
2	3	400	2.0e-2	2.7e-1	8.6e-2	2.8e-3	2.9e-2	1.6e-2
3	4	679	6.1e-3	7.4e-2	2.5e-2	8.3e-4	7.0e-3	4.3e-3
4	4	1711	1.7e-3	2.0e-2	7.5e-3	3.7e-4	2.1e-3	1.5e-3
5	6	5743	4.6e-4	5.1e-3	2.5e-3	1.4e-4	6.4e-4	5.3e-4
6	6	20974	1.2e-4	1.9e-3	1.9e-3	5.5e-5	2.2e-4	2.0e-4
$\gamma = 0.05$								
2	3	400	2.0e-2	2.7e-1	8.6e-2	2.8e-3	2.9e-2	1.6e-2
3	4	751	5.8e-3	7.2e-2	2.4e-2	7.3e-4	6.6e-3	4.0e-3
4	4	1969	1.6e-3	1.9e-2	6.6e-3	2.5e-4	1.7e-3	1.2e-3
5	5	6694	4.2e-4	4.8e-3	1.7e-3	9.1e-5	4.9e-4	3.7e-4
6	6	22544	1.1e-4	1.2e-3	5.1e-4	3.4e-5	1.5e-4	1.3e-4
$\gamma = 0.025$								
2	3	400	2.0e-2	2.7e-1	8.6e-2	2.8e-3	2.9e-2	1.6e-2
3	3	775	5.8e-3	7.1e-2	2.4e-2	7.2e-4	6.6e-3	4.0e-3
4	3	2161	1.6e-3	1.8e-2	6.5e-3	2.0e-4	1.6e-3	1.1e-3
5	5	7486	4.1e-4	4.6e-3	1.7e-3	6.3e-5	4.2e-4	2.9e-4
6	5	28165	1.0e-4	1.2e-3	4.3e-4	2.1e-5	1.2e-4	8.9e-5

Table 15: MG-AR performance, MFE error indicator, $m = 0$.

st	sw	CVs	$\| e_0 \|_C$	$\| e_1 \|_C$	$\| e_2 \|_C$	$\| e_0 \|_{L_2}$	$\| e_1 \|_{L_2}$	$\| e_2 \|_{L_2}$
$\gamma = 0.1$								
2	3	400	2.0e-2	2.7e-1	8.6e-2	2.8e-3	2.9e-2	1.6e-2
3	3	727	5.9e-3	7.2e-2	2.4e-2	7.4e-4	6.7e-3	4.1e-3
4	4	1924	1.6e-3	1.9e-2	9.4e-3	2.6e-4	1.8e-3	1.3e-3
5	5	6331	6.0e-4	7.6e-3	5.9e-3	1.3e-4	7.6e-4	6.1e-4
6	7	23362	1.9e-4	2.5e-3	2.2e-3	4.8e-5	2.5e-4	2.1e-4
$\gamma = 0.05$								
2	3	400	2.0e-2	2.7e-1	8.6e-2	2.8e-3	2.9e-2	1.6e-2
3	5	769	5.8e-3	7.1e-2	2.4e-2	7.3e-4	6.6e-3	4.1e-3
4	5	2113	1.6e-3	1.8e-2	6.9e-3	2.1e-4	1.7e-3	1.1e-3
5	4	7171	4.1e-4	4.6e-3	2.7e-3	7.5e-5	4.5e-4	3.3e-4
6	6	26773	1.4e-4	1.4e-3	1.1e-3	2.8e-5	1.6e-4	1.3e-4
$\gamma = 0.025$								
2	3	400	2.0e-2	2.7e-1	8.6e-2	2.8e-3	2.9e-2	1.6e-2
3	4	802	5.8e-3	7.1e-2	2.4e-2	7.2e-4	6.6e-3	4.0e-3
4	5	2248	1.5e-3	1.8e-2	6.4e-3	2.0e-4	1.6e-3	1.1e-3
5	6	7885	4.0e-4	4.5e-3	1.8e-3	5.7e-5	4.1e-4	2.9e-4
6	5	29578	1.1e-4	1.2e-3	6.7e-4	1.9e-5	1.2e-4	8.7e-5

Table 16: MG-AR performance, FE error indicator, $m = 0.5$.

st	sw	CVs	$\| e_0 \|_C$	$\| e_1 \|_C$	$\| e_2 \|_C$	$\| e_0 \|_{L_2}$	$\| e_1 \|_{L_2}$	$\| e_2 \|_{L_2}$
$\gamma = 0.2$								
2	5	400	1.2e-1	3.6e+0	1.9e+0	2.4e-2	4.2e-1	2.9e-1
3	9	625	4.2e-2	1.3e+0	6.0e-1	1.2e-2	1.3e-1	8.9e-2
4	8	1402	1.4e-2	4.7e-1	1.9e-1	4.9e-3	4.2e-2	2.9e-2
5	15	4189	5.1e-3	1.8e-1	6.2e-2	2.1e-3	1.4e-2	9.7e-3
6	9	14863	1.8e-3	7.0e-2	2.1e-2	8.5e-4	5.0e-3	3.3e-3
$\gamma = 0.1$								
2	5	400	1.2e-1	3.6e+0	1.9e+0	2.4e-2	4.2e-1	2.9e-1
3	8	679	4.1e-2	1.3e+0	5.9e-1	1.1e-2	1.3e-1	8.8e-2
4	7	1690	1.4e-2	4.7e-1	1.9e-1	4.6e-3	4.1e-2	2.8e-2
5	9	5422	5.0e-3	1.8e-1	6.1e-2	1.9e-3	1.4e-2	9.3e-3
6	11	20026	1.8e-3	6.9e-2	2.0e-2	7.7e-4	4.8e-3	3.1e-3
$\gamma = 0.05$								
2	5	400	1.2e-1	3.6e+0	1.9e+0	2.4e-2	4.2e-1	2.9e-1
3	7	706	4.1e-2	1.3e+0	5.9e-1	1.0e-2	1.3e-1	8.8e-2
4	8	1867	1.4e-2	4.7e-1	1.9e-1	4.2e-3	4.1e-2	2.8e-2
5	8	6250	4.9e-3	1.8e-1	6.0e-2	1.7e-3	1.4e-2	9.2e-3
6	11	23287	1.7e-3	6.8e-2	2.0e-2	6.7e-4	4.7e-3	3.1e-3

Table 17: MG-AR performance, MFE error indicator, $m = 0.5$.

st	sw	CVs	$\| e_0 \|_C$	$\| e_1 \|_C$	$\| e_2 \|_C$	$\| e_0 \|_{L_2}$	$\| e_1 \|_{L_2}$	$\| e_2 \|_{L_2}$
$\gamma = 0.2$								
2	5	400	1.2e-1	3.6e+0	1.9e+0	2.4e-2	4.2e-1	2.9e-1
3	9	643	4.2e-2	1.3e+0	6.0e-1	1.2e-2	1.3e-1	8.9e-2
4	14	1606	1.4e-2	4.7e-1	1.9e-1	4.9e-3	4.2e-2	2.8e-2
5	11	5410	5.0e-3	1.8e-1	6.1e-2	1.9e-3	1.4e-2	9.4e-3
6	10	19453	1.9e-3	7.3e-2	2.3e-2	8.4e-4	5.3e-3	3.5e-3
$\gamma = 0.1$								
2	5	400	1.2e-1	3.6e+0	1.9e+0	2.4e-2	4.2e-1	2.9e-1
3	8	700	4.1e-2	1.3e+0	5.9e-1	1.0e-2	1.3e-1	8.8e-2
4	9	1849	1.4e-2	4.7e-1	1.9e-1	4.3e-3	4.1e-2	2.8e-2
5	10	6367	4.9e-3	1.8e-1	6.0e-2	1.7e-3	1.4e-2	9.2e-3
6	10	23542	1.7e-3	6.9e-2	2.0e-2	6.8e-4	4.7e-3	3.1e-3
$\gamma = 0.05$								
2	5	400	1.2e-1	3.6e+0	1.9e+0	2.4e-2	4.2e-1	2.9e-1
3	6	727	4.1e-2	1.3e+0	5.9e-1	1.0e-2	1.3e-1	8.8e-2
4	10	2050	1.4e-2	4.6e-1	1.9e-1	4.1e-3	4.1e-2	2.8e-2
5	10	7216	4.8e-3	1.7e-1	6.0e-2	1.6e-3	1.4e-2	9.1e-3
6	11	26896	1.7e-3	6.8e-2	2.0e-2	6.2e-4	4.6e-3	3.1e-3

Table 18: MG-AR performance, FE error indicator, $m = 1$.

st	sw	CVs	$\| e_0 \|_C$	$\| e_1 \|_C$	$\| e_2 \|_C$	$\| e_0 \|_{L_2}$	$\| e_1 \|_{L_2}$	$\| e_2 \|_{L_2}$
$\gamma = 0.1$								
2	17	400	1.2e-1	8.4e+0	5.9e+0	2.7e-2	1.0e+0	8.4e-1
3	20	670	3.4e-2	2.5e+0	1.7e+0	1.1e-2	2.5e-1	2.0e-1
4	21	1591	1.0e-2	7.5e-1	4.4e-1	4.8e-3	6.4e-2	5.0e-2
5	24	5086	4.0e-3	2.0e-1	1.1e-1	1.9e-3	1.7e-2	1.3e-2
6	27	18601	1.5e-3	5.2e-2	3.0e-2	6.9e-4	4.3e-3	3.4e-3
$\gamma = 0.05$								
2	17	400	1.2e-1	8.4e+0	5.9e+0	2.7e-2	1.0e+0	8.4e-1
3	20	688	3.3e-2	2.5e+0	1.7e+0	1.0e-2	2.5e-1	2.0e-1
4	21	1777	9.4e-3	7.3e-1	4.3e-1	3.7e-3	6.3e-2	4.9e-2
5	24	5818	2.9e-3	1.9e-1	1.1e-1	1.4e-3	1.6e-2	1.3e-2
6	27	21574	1.0e-3	4.9e-2	2.9e-2	4.9e-4	4.0e-3	3.2e-3
$\gamma = 0.025$								
2	17	400	1.2e-1	8.4e+0	5.9e+0	2.7e-2	1.0e+0	8.4e-1
3	20	721	3.3e-2	2.5e+0	1.7e+0	9.7e-3	2.5e-1	2.0e-1
4	21	1906	9.2e-3	7.2e-1	4.3e-1	3.3e-3	6.2e-2	4.9e-2
5	24	5373	2.6e-3	1.9e-1	1.1e-1	1.1e-3	1.6e-2	1.2e-2
6	27	23839	7.9e-4	4.8e-2	2.8e-2	3.8e-4	3.9e-3	3.2e-3

Table 19: MG-AR performance, MFE error indicator, $m = 1$.

st	sw	CVs	$\| e_0 \|_C$	$\| e_1 \|_C$	$\| e_2 \|_C$	$\| e_0 \|_{L_2}$	$\| e_1 \|_{L_2}$	$\| e_2 \|_{L_2}$
$\gamma = 0.1$								
2	17	400	1.2e-1	8.4e+0	5.9e+0	2.7e-2	1.0e+0	8.4e-1
3	19	655	3.4e-2	2.6e+0	1.7e+0	1.1e-2	2.5e-1	2.0e-1
4	21	1726	9.8e-3	7.4e-1	4.3e-1	4.0e-3	6.3e-2	5.0e-2
5	24	5971	3.1e-3	1.9e-1	1.1e-1	1.3e-3	1.6e-2	1.3e-2
6	27	22453	1.2e-3	4.9e-2	2.9e-2	4.3e-4	4.0e-3	3.2e-3
$\gamma = 0.05$								
2	17	400	1.2e-1	8.4e+0	5.9e+0	2.7e-2	1.0e+0	8.4e-1
3	20	706	3.3e-2	2.5e+0	1.7e+0	9.7e-3	2.5e-1	2.0e-1
4	21	1909	9.2e-3	7.2e-1	4.3e-1	3.4e-3	6.2e-2	4.9e-2
5	24	6880	2.6e-3	1.9e-1	1.1e-1	1.1e-3	1.6e-2	1.2e-2
6	27	26209	7.6e-4	4.8e-2	2.8e-2	3.2e-4	3.9e-3	3.2e-3
$\gamma = 0.025$								
2	17	400	1.2e-1	8.4e+0	5.9e+0	2.7e-2	1.0e+0	8.4e-1
3	20	742	3.3e-2	2.5e+0	1.7e+0	9.5e-3	2.5e-1	2.0e-1
4	21	2107	9.0e-3	7.2e-1	4.3e-1	3.1e-3	6.2e-2	4.9e-2
5	24	7657	2.5e-3	1.9e-1	1.1e-1	9.6e-4	1.6e-2	1.2e-2
6	27	29317	6.8e-4	4.7e-2	2.8e-2	2.9e-4	3.9e-3	3.1e-3

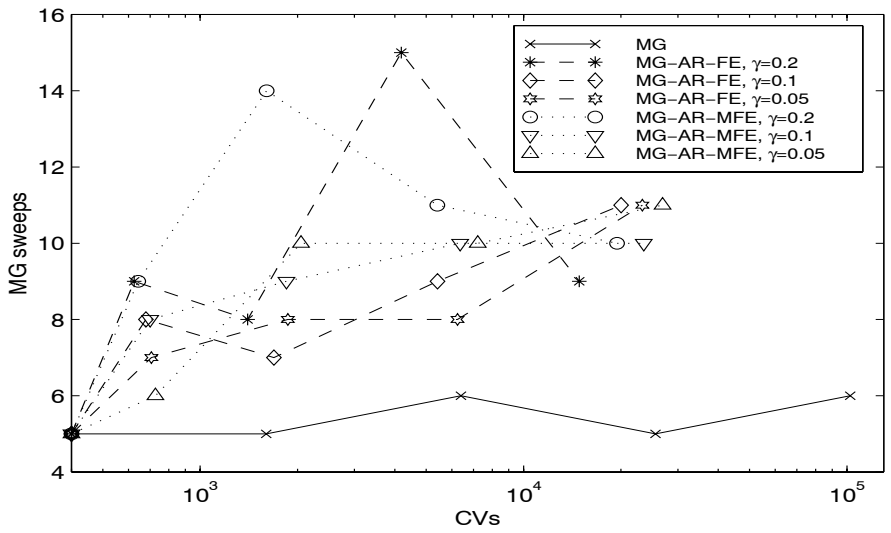

Figure 9: Dependence of the number of MG sweeps on the number of CVs for MG and MG-AR, using FE and MFE error indicators, $m = 0.5$.

well as on the degree of nonlinearity of the problem.

Example 3. In this example we compute the pressure distribution in a porous medium with parameters $K_1 = K_2 = 1$, $m = 0.5$. The pressure is prescribed as $p = 0$ at $y = 0$, $0 \leq x \leq 0.1$ (outflow) and as $p = 1$ at $y = 1$, $0.9 \leq x \leq 1$ (inflow). On the other part of the boundary homogenous Neumann boundary condition for the pressure is prescribed (solid walls). Some results are presented in Table 20. In the first column the number of the corresponding level of refinement 'st' is given, in the next three columns results for multigrid with global refinement are presented – the number of nonlinear multigrid iterations 'sw', the number of CVs and the discrete maximum-norm $\| p - p_f \|_C$ of the difference between the multigrid solution on the corresponding grid p and the restricted global solution from the finest grid p_f. In the next six columns similar data for multigrid adaptive-refinement solution p using the finite element error indicator (3) and the mixed finite element error indicator (4) are presented. Note, the global finest grid solution p_f is restricted on the corresponding composite grid in the case of adaptive refinement. As it can be seen, on the coarser grids $\| p - p_f \|_C$ is one and the same in the cases of global and adaptive refinement solution, on the finest grid $\| p - p_f \|_C$ in the case of adaptive refinement is much smaller than this difference on the coarser grids, i.e., the adaptive refinement solution is really improved on the last grid. On the other side, a lot of computational work is avoided in the case of adaptive refinement.

The final composite grids for the MG-AR algorithm are shown on Fig. 14. The left column is for the FE error indicator, the right is for the MFE error indicator. In both

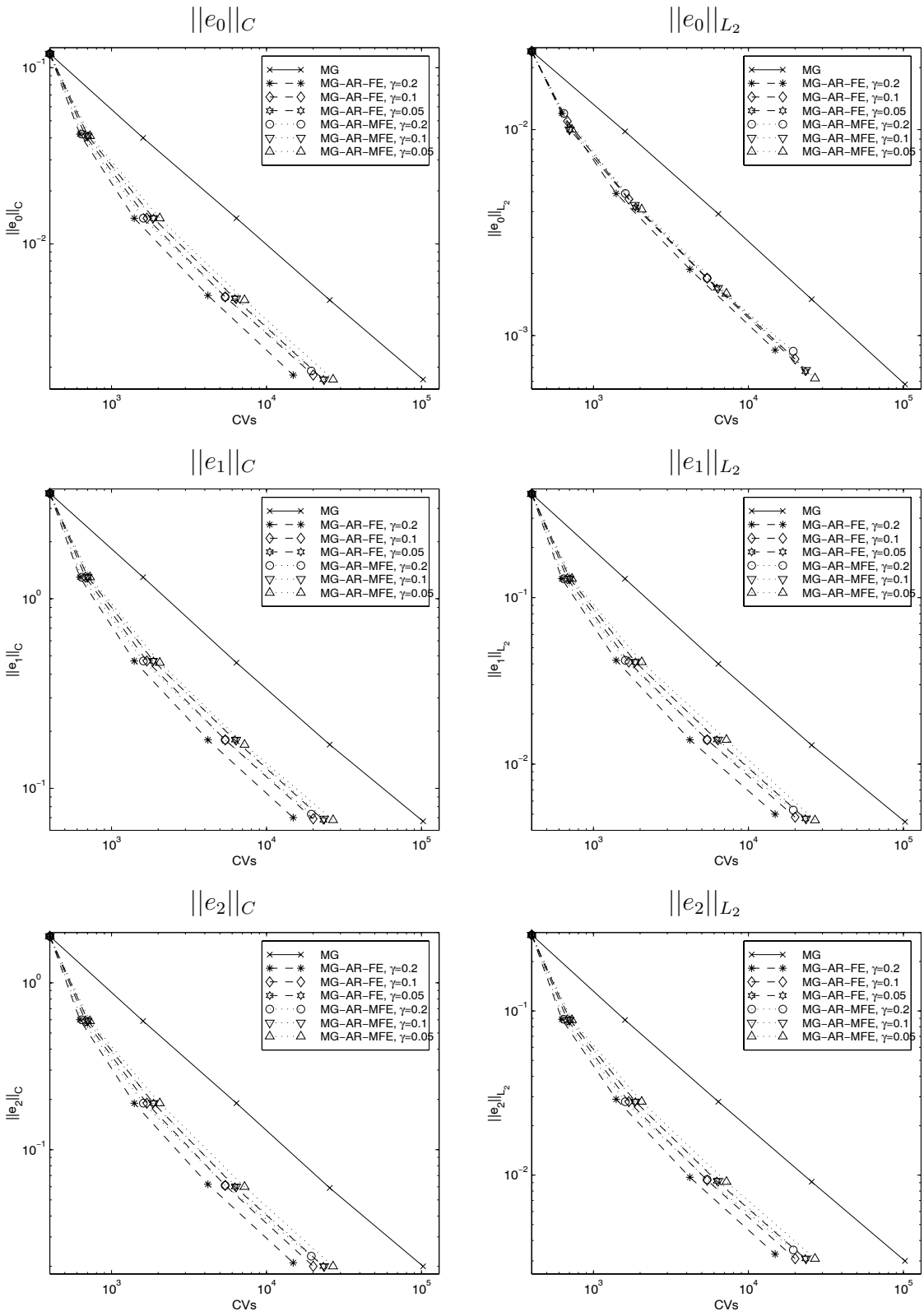

Figure 10: Dependence of the solution accuracy on the number of CVs for MG and MG-AR, using FE and MFE error indicators, $m = 0.5$.

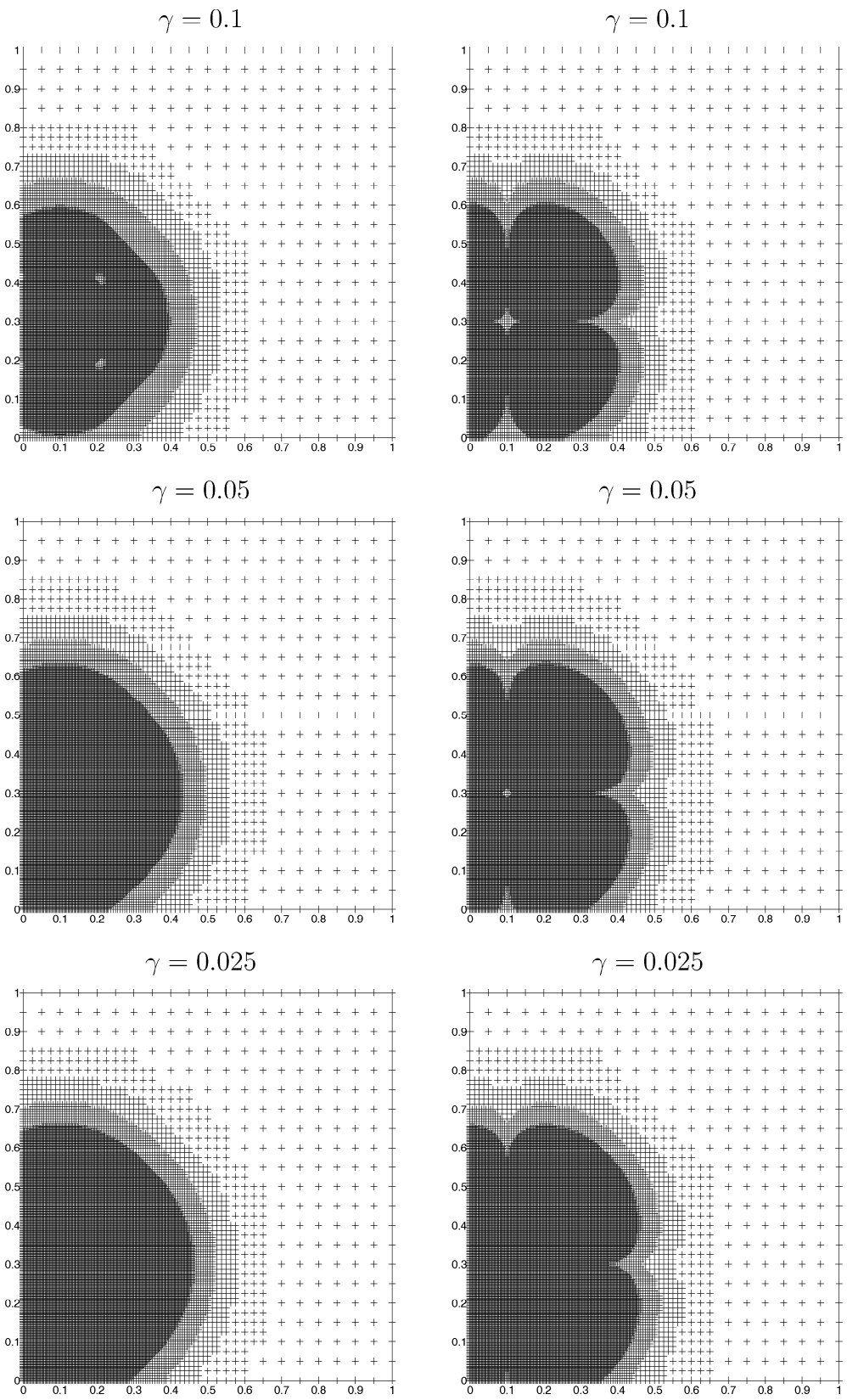

Figure 11: Final composite grids, left – using FE error indicator, right – using MFE error indicator, $m = 0$.

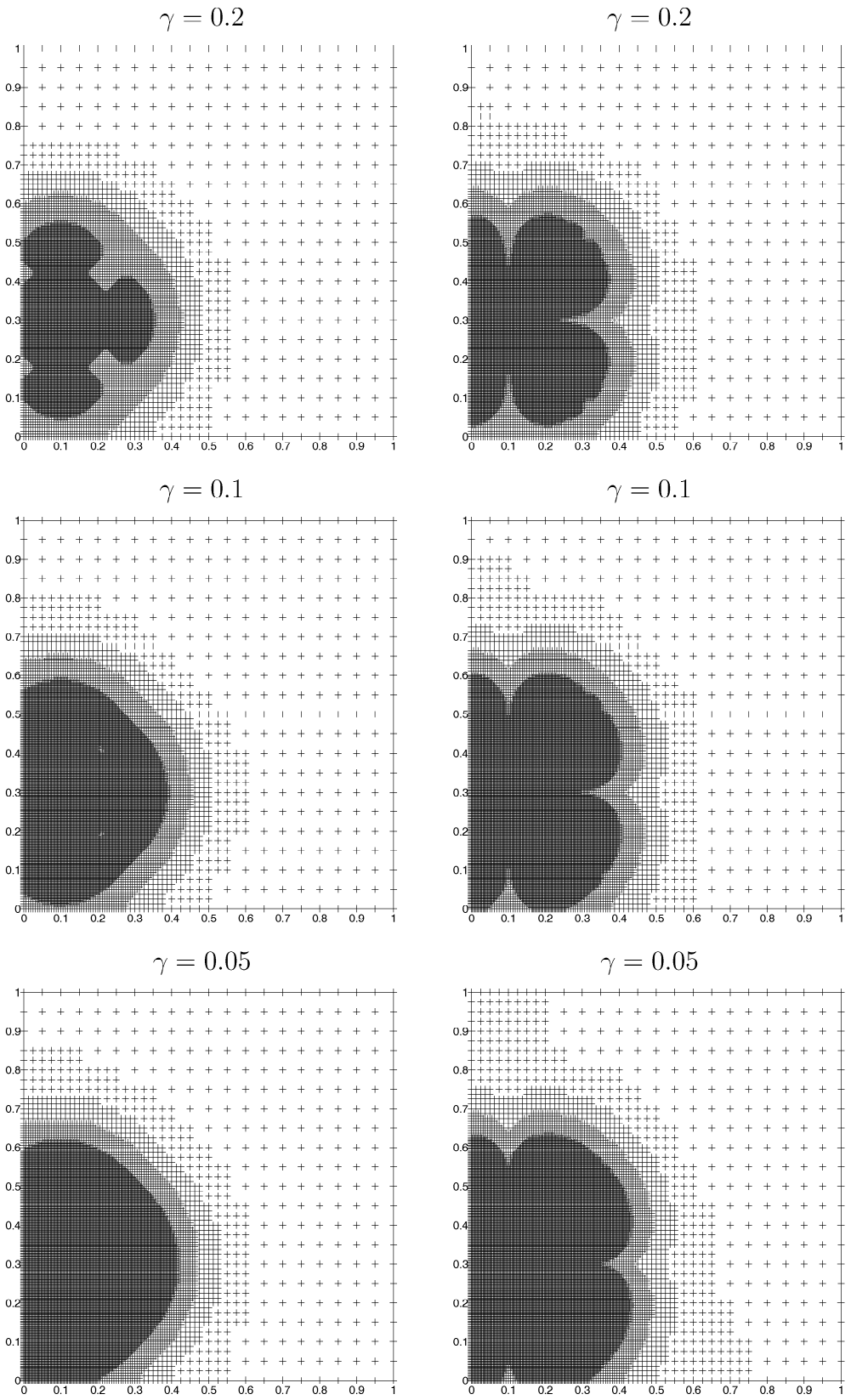

Figure 12: Final composite grids, left – using FE error indicator, right – using MFE error indicator, $m = 0.5$.

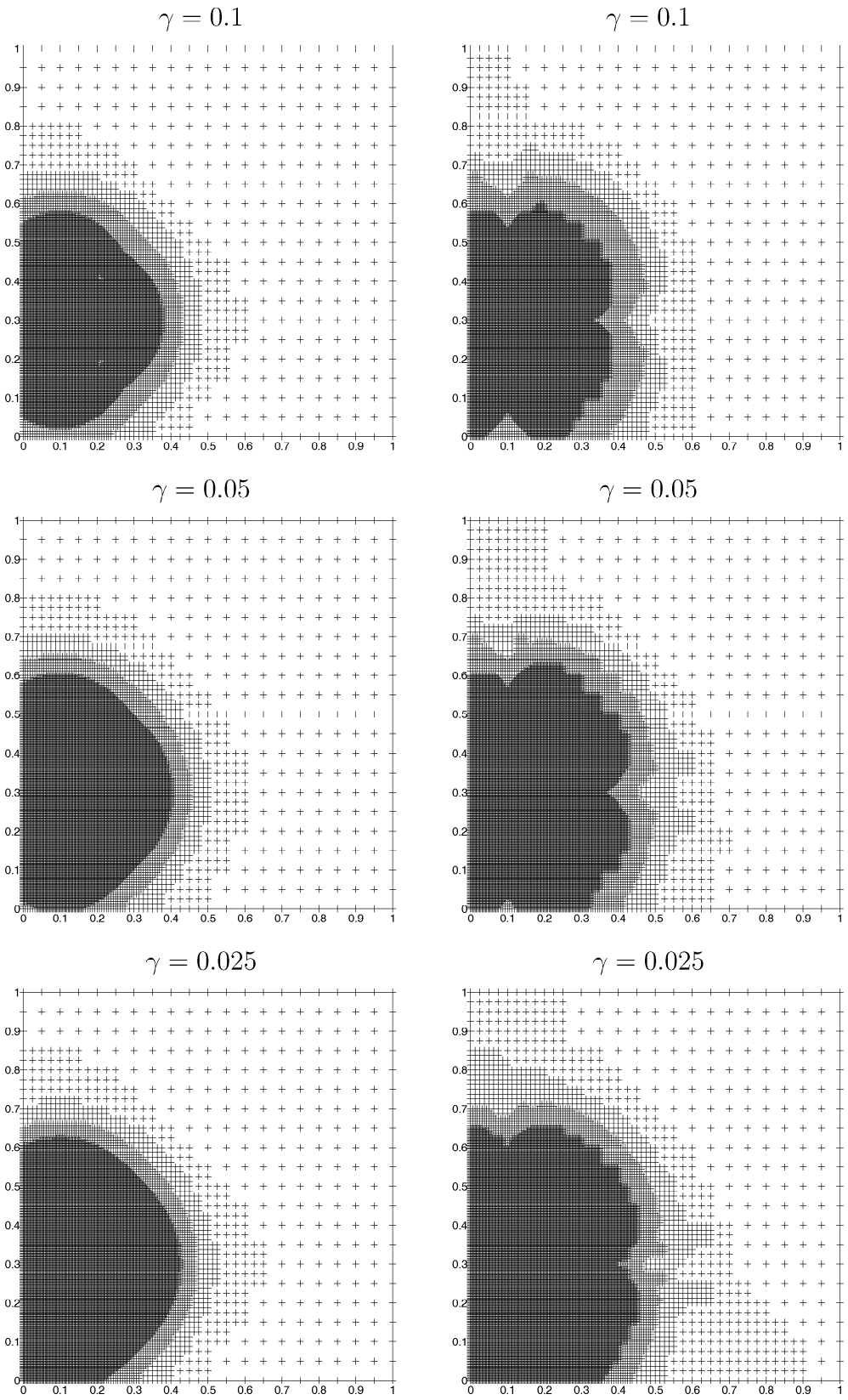

Figure 13: Final composite grids, left – using FE error indicator, right – using MFE error indicator, $m = 1$.

Table 20: Difference between the restricted global finest grid solution and the current solution.

	global solution			AR sol., FE error ind.			AR sol., MFE error ind.		
st	sw	CVs	$\| p - p_f \|_C$	sw	CVs	$\| p - p_f \|_C$	sw	CVs	$\| p - p_f \|_C$
					$\gamma = 0.5$				
2	5	400	8.0e-3	5	400	8.0e-3	5	400	8.0e-3
3	5	1600	4.9e-3	8	466	4.9e-3	9	442	4.9e-3
4	6	6400	2.8e-3	8	592	2.8e-3	9	508	2.8e-3
5	6	25600	1.2e-3	8	760	1.2e-3	9	622	1.2e-3
6	6	102400	0	8	994	3.1e-4	9	784	3.4e-4
					$\gamma = 0.2$				
2	5	400	8.0e-3	5	400	8.0e-3	5	400	8.0e-3
3	5	1600	4.9e-3	6	550	4.9e-3	7	502	4.9e-3
4	6	6400	2.8e-3	7	814	2.8e-3	8	640	2.8e-3
5	6	25600	1.2e-3	7	1204	1.2e-3	8	844	1.2e-3
6	6	102400	0	7	1936	1.5e-4	8	1144	2.8e-4
					$\gamma = 0.1$				
2	5	400	8.0e-3	5	400	8.0e-3	5	400	8.0e-3
3	5	1600	4.9e-3	6	712	4.9e-3	6	568	4.9e-3
4	6	6400	2.8e-3	6	1492	2.8e-3	7	838	2.8e-3
5	6	25600	1.2e-3	6	2260	1.2e-3	6	1270	1.2e-3
6	6	102400	0	6	3154	9.3e-5	7	1840	2.4e-4

cases the grid is properly refined near the boundary between the inlet/outlet and the wall, where the flow direction and the pressure change most rapidly.

Example 4. Some results for the computation of the pressure distribution in a porous medium with the same parameters, as in Example 3, but with an outflow at $y = 0$, $0.05 \leq x \leq 0.2$, are presented in Table 21. As in the previous example, on the coarser grids $\| p - p_f \|_C$ is one and the same in the cases of global and adaptive refinement solution, on the finest grid $\| p - p_f \|_C$ in the case of adaptive refinement is much smaller then this difference on the coarser grids, i.e., the adaptive refinement solution has really improved on the last grid. On the other side, a lot of computational work is avoided in the case of adaptive refinement.
The final composite grids for the MG-AR algorithm are shown on Fig. 15. In all cases the grid is properly refined near the boundaries between the inlet/outlet and the wall, where the flow direction and the pressure change most rapidly.

5 Concluding remarks

A MG-ALR solver for non-Newtonian flow in porous media is presented. The numerical experiments demonstrate that the adaptive local refinement approach allows to obtain the same accuracy as in the full grid case, but using significantly less memory and CPU time. The both error indicators studied, show similar behaviour, both of them can be further used in practical computations. The numerical results show the efficiency of the multigrid approach: even in the strongly nonlinear cases, the amount of computations is almost proportional to the number of CVs.
Second order accuracy is ensured not only for the pressure, but also for the fluxes. This is a result of a proper approximation for the slave nodes on the interface between the coarse and the fine grids, as well as of a proper discretization at the near boundary cells in the case of Dirichlet boundary conditions.

Acknowledgments. D. Vassileva acknowledges the fellowship from European Research Consortium for Informatics and Mathematics (ERCIM) for her work at ITWM, Kaiserslautern.

References

[1] Brandt, A.: Multi-level adaptive solutions to boundary value problems. Math. Comp. **31** (1977), 333–390.

[2] Bai, D., Brandt, A.: Local mesh refinement multilevel techniques. SIAM J. Sci. Stat. Comput. **8** (1987), 109–134.

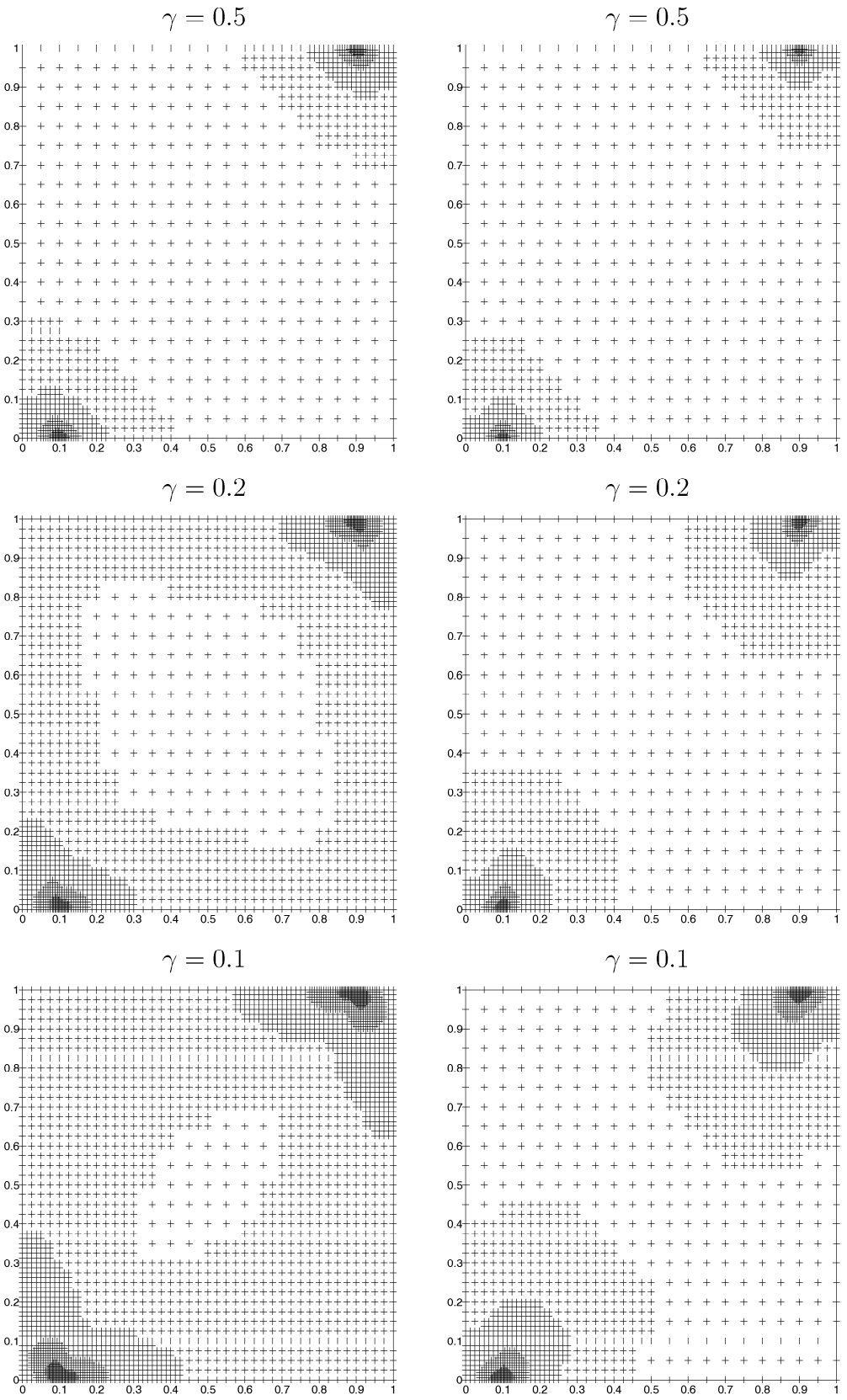

Figure 14: Final composite grids, left – using FE error indicator, right – using MFE error indicator.

Table 21: Difference between the restricted global finest grid solution and the current solution.

	global solution			AR sol., FE error ind.			AR sol., MFE error ind.		
st	sw	CVs	$\| p - p_f \|_C$	sw	CVs	$\| p - p_f \|_C$	sw	CVs	$\| p - p_f \|_C$
					$\gamma = 0.5$				
2	7	400	8.8e-3	7	400	8.8e-3	7	400	8.8e-3
3	7	1600	5.3e-3	10	466	5.3e-3	9	454	5.3e-3
4	7	6400	3.0e-3	9	577	3.0e-3	10	547	3.0e-3
5	6	25600	1.3e-3	9	760	1.3e-3	11	691	1.3e-3
6	6	102400	0	10	1021	8.3e-4	11	898	3.1e-4
					$\gamma = 0.2$				
2	7	400	8.8e-3	7	400	8.8e-3	7	400	8.8e-3
3	7	1600	5.3e-3	7	553	5.3e-3	8	502	5.3e-3
4	7	6400	3.0e-3	7	826	3.0e-3	8	658	3.0e-3
5	6	25600	1.3e-3	8	1234	1.3e-3	8	898	1.3e-3
6	6	102400	0	9	2023	1.3e-4	8	1249	2.6e-4
					$\gamma = 0.1$				
2	7	400	8.8e-3	7	400	8.8e-3	7	400	8.8e-3
3	7	1600	5.3e-3	7	709	5.3e-3	8	568	5.3e-3
4	7	6400	3.0e-3	7	1468	3.0e-3	8	853	3.0e-3
5	6	25600	1.3e-3	7	2257	1.3e-3	8	1291	1.3e-3
6	6	102400	0	7	3163	8.5e-5	8	1891	2.2e-4

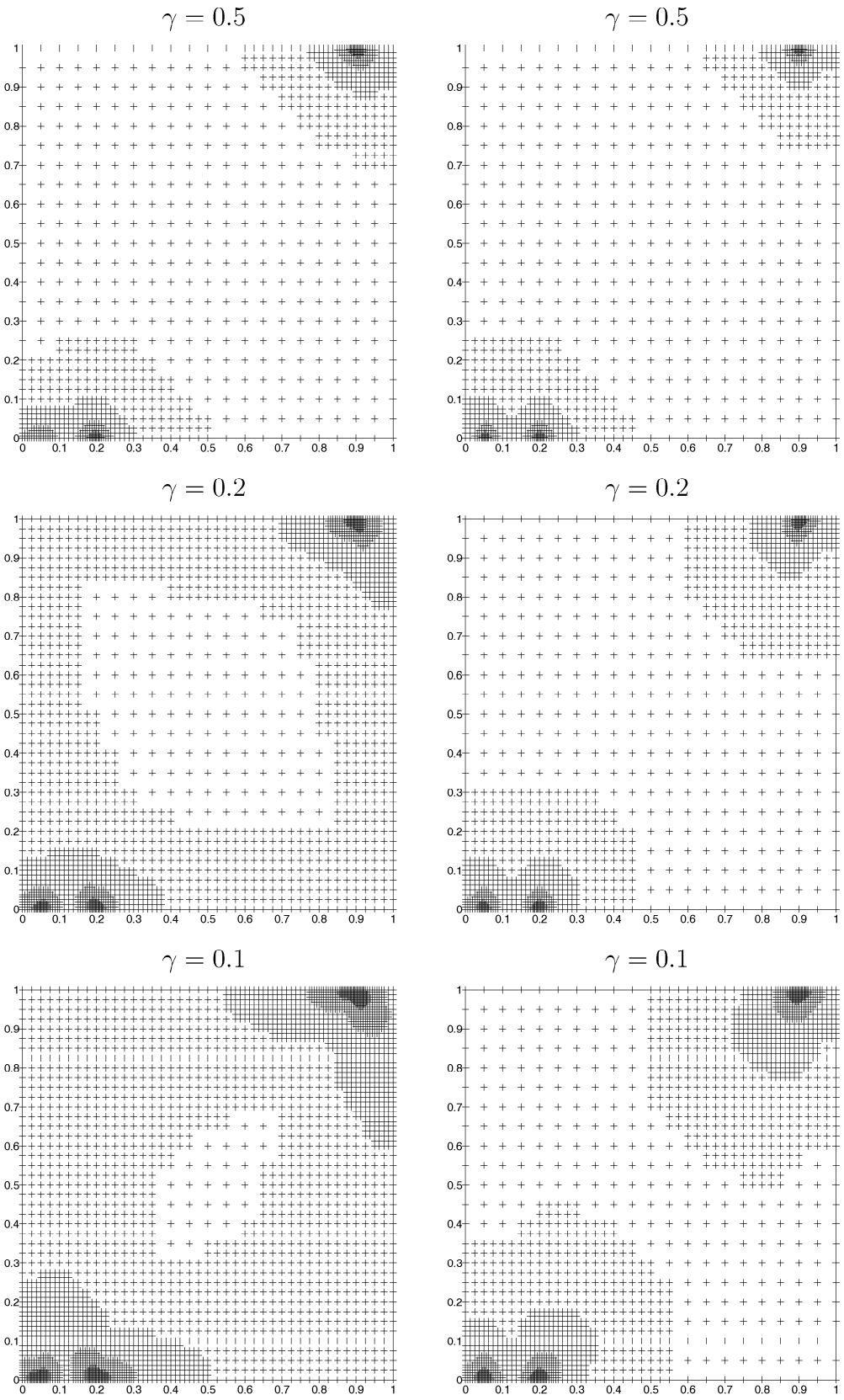

Figure 15: Final composite grids, left – using FE error indicator, right – using MFE error indicator.

[3] McCormick, S. F.: Multilevel Adaptive Methods for Partial Differential Equations. SIAM, Philadelphia (1989).

[4] Verfürth, R.: A Review of a Posteriori Error Estimators and Adaptive Mesh Refinement Techniques. Teubner-Wiley, Stuttgart (1996).

[5] Ewing, R., Lazarov, R., Vassilevski, P.: Local refinement techniques for elliptic problems on cell-centered grids I. Error analysis. Math. Comp. **56** (1991), 437–461.

[6] Ewing, R., Lazarov, R., Vassilevski, P.: Local refinement techniques for elliptic problems on cell-centered grids II: Optimal order two-grid iterative methods. Numer. Linear Algebra Appl. **1** (1994), 337–368.

[7] Babuška, I., Rheinboldt, W.C.: Error estimates for adaptive finite element computations. SIAM J. Numer. Anal. **15** (1978), 736–754.

[8] Bank, R.E., Weiser, A.: Some a posteriori error estimators for elliptic partial differential equations. Math. Comput. **44** (1985), 283–305.

[9] Zienkiewicz, O.C., Zhu, J.Z.: A simple error estimator and adaptive procedure for practical engineering analysis. Internat. J. Numer. Meth. Engrg. **24** (1987), 337–357.

[10] Ainsworth, M., Oden, J.T.: A Posteriori Error Estimation in Finite Element Analysis. Pure and Appl. Math., Wiley, Chichester (2000).

[11] Dörfler, W.: A convergent adaptive algorithm for Poisson equation. SIAM J. Numer. Anal. **33** (1996), 1106–1122.

[12] Dörfler, W., Wilderotter, O.: An adaptive algorithm finite element method for a linear elliptic equation with variable coefficients. Z. Angew. Math. Mech. **80** (2000), 481–491.

[13] Carstensen, C.: A posteriori error estimate for the mixed finite element method. Math. Comp. **66** (1997), 465–476.

[14] Wohlmuth, B., Hoppe, R.: A comparison of a posteriori error estimators for mixed finite element discretizations by Raviart-Thomas elements. Math. Comput. **68** (1999), 1347–1378.

[15] Lazarov, R., Tomov, S.: A posteriori error estimates for finite volume element approximations of convection-diffusion-reaction equations. Comput. Geosciences **6** (2002), 483–503.

[16] Wesseling, P.: Uniform convergence of discretization error for a singular perturbation problem. Numer. Meth. Partial Diff. Equations **12** (1996), 657–671.

[17] Iliev, O.: On second-order-accurate discretization of 3D interface problems and its fast solution with a pointwise multigrid solver. IMA J. Numer. Anal. **22** (2002), 391–406.

[18] Greenkorn, R.: Flow Phenomena in Porous Media. Marcel Dekker Inc., New York (1983).

[19] Hackbusch, W.: Multi-Grid Methods and Applications. Springer, Berlin (1985).

[20] Wesseling, P.: An Introduction to Multigrid Methods. Wiley, New York (1991).

[21] Iliev, O., Stoyanov, D.: On a multigrid local refinement solver for incompressible Navier-Stokes equations. Math. Model. **13** (2001), 95–106.

[22] Iliev, O., Stoyanov, D.: Multigrid adaptive local refinement solvers for incompressible flows. *In* Large-Scale Scientific Computing, eds. Margenov, S. et al., Lect. Notes Comp. Sci. **2179**, 361–368.

[23] Tucker, C., Dessenberger R.: Governing equations for flow and heat transfer in stationary fiber beds, *In* Flow and rheology in polymer composite manufacturing, eds. Advani, S.G. et al, Elsevier (1994), 257–324.

Published reports of the Fraunhofer ITWM

The PDF-files of the following reports are available under:
www.itwm.fraunhofer.de/de/zentral__berichte/berichte

1. D. Hietel, K. Steiner, J. Struckmeier

A Finite - Volume Particle Method for Compressible Flows

We derive a new class of particle methods for conservation laws, which are based on numerical flux functions to model the interactions between moving particles. The derivation is similar to that of classical Finite-Volume methods; except that the fixed grid structure in the Finite-Volume method is substituted by so-called mass packets of particles. We give some numerical results on a shock wave solution for Burgers equation as well as the well-known one-dimensional shock tube problem.
(19 pages, 1998)

2. M. Feldmann, S. Seibold

Damage Diagnosis of Rotors: Application of Hilbert Transform and Multi-Hypothesis Testing

In this paper, a combined approach to damage diagnosis of rotors is proposed. The intention is to employ signal-based as well as model-based procedures for an improved detection of size and location of the damage. In a first step, Hilbert transform signal processing techniques allow for a computation of the signal envelope and the instantaneous frequency, so that various types of non-linearities due to a damage may be identified and classified based on measured response data. In a second step, a multi-hypothesis bank of Kalman Filters is employed for the detection of the size and location of the damage based on the information of the type of damage provided by the results of the Hilbert transform.
Keywords: Hilbert transform, damage diagnosis, Kalman filtering, non-linear dynamics
(23 pages, 1998)

3. Y. Ben-Haim, S. Seibold

Robust Reliability of Diagnostic Multi-Hypothesis Algorithms: Application to Rotating Machinery

Damage diagnosis based on a bank of Kalman filters, each one conditioned on a specific hypothesized system condition, is a well recognized and powerful diagnostic tool. This multi-hypothesis approach can be applied to a wide range of damage conditions. In this paper, we will focus on the diagnosis of cracks in rotating machinery. The question we address is: how to optimize the multi-hypothesis algorithm with respect to the uncertainty of the spatial form and location of cracks and their resulting dynamic effects. First, we formulate a measure of the reliability of the diagnostic algorithm, and then we discuss modifications of the diagnostic algorithm for the maximization of the reliability. The reliability of a diagnostic algorithm is measured by the amount of uncertainty consistent with no-failure of the diagnosis. Uncertainty is quantitatively represented with convex models.
Keywords: Robust reliability, convex models, Kalman filtering, multi-hypothesis diagnosis, rotating machinery, crack diagnosis
(24 pages, 1998)

4. F.-Th. Lentes, N. Siedow

Three-dimensional Radiative Heat Transfer in Glass Cooling Processes

For the numerical simulation of 3D radiative heat transfer in glasses and glass melts, practically applicable mathematical methods are needed to handle such problems optimal using workstation class computers. Since the exact solution would require super-computer capabilities we concentrate on approximate solutions with a high degree of accuracy. The following approaches are studied: 3D diffusion approximations and 3D ray-tracing methods.
(23 pages, 1998)

5. A. Klar, R. Wegener

A hierarchy of models for multilane vehicular traffic
Part I: Modeling

In the present paper multilane models for vehicular traffic are considered. A microscopic multilane model based on reaction thresholds is developed. Based on this model an Enskog like kinetic model is developed. In particular, care is taken to incorporate the correlations between the vehicles. From the kinetic model a fluid dynamic model is derived. The macroscopic coefficients are deduced from the underlying kinetic model. Numerical simulations are presented for all three levels of description in [10]. Moreover, a comparison of the results is given there.
(23 pages, 1998)

Part II: Numerical and stochastic investigations

In this paper the work presented in [6] is continued. The present paper contains detailed numerical investigations of the models developed there. A numerical method to treat the kinetic equations obtained in [6] are presented and results of the simulations are shown. Moreover, the stochastic correlation model used in [6] is described and investigated in more detail.
(17 pages, 1998)

6. A. Klar, N. Siedow

Boundary Layers and Domain Decomposition for Radiative Heat Transfer and Diffusion Equations: Applications to Glass Manufacturing Processes

In this paper domain decomposition methods for radiative transfer problems including conductive heat transfer are treated. The paper focuses on semi-transparent materials, like glass, and the associated conditions at the interface between the materials. Using asymptotic analysis we derive conditions for the coupling of the radiative transfer equations and a diffusion approximation. Several test cases are treated and a problem appearing in glass manufacturing processes is computed. The results clearly show the advantages of a domain decomposition approach. Accuracy equivalent to the solution of the global radiative transfer solution is achieved, whereas computation time is strongly reduced.
(24 pages, 1998)

7. I. Choquet

Heterogeneous catalysis modelling and numerical simulation in rarified gas flows Part I: Coverage locally at equilibrium

A new approach is proposed to model and simulate numerically heterogeneous catalysis in rarefied gas flows. It is developed to satisfy all together the following points:
1) describe the gas phase at the microscopic scale, as required in rarefied flows,
2) describe the wall at the macroscopic scale, to avoid prohibitive computational costs and consider not only crystalline but also amorphous surfaces,
3) reproduce on average macroscopic laws correlated with experimental results and
4) derive analytic models in a systematic and exact way. The problem is stated in the general framework of a non static flow in the vicinity of a catalytic and non porous surface (without aging). It is shown that the exact and systematic resolution method based on the Laplace transform, introduced previously by the author to model collisions in the gas phase, can be extended to the present problem. The proposed approach is applied to the modelling of the EleyRideal and LangmuirHinshelwood recombinations, assuming that the coverage is locally at equilibrium. The models are developed considering one atomic species and extended to the general case of several atomic species. Numerical calculations show that the models derived in this way reproduce with accuracy behaviors observed experimentally.
(24 pages, 1998)

8. J. Ohser, B. Steinbach, C. Lang

Efficient Texture Analysis of Binary Images

A new method of determining some characteristics of binary images is proposed based on a special linear filtering. This technique enables the estimation of the area fraction, the specific line length, and the specific integral of curvature. Furthermore, the specific length of the total projection is obtained, which gives detailed information about the texture of the image. The influence of lateral and directional resolution depending on the size of the applied filter mask is discussed in detail. The technique includes a method of increasing directional resolution for texture analysis while keeping lateral resolution as high as possible.
(17 pages, 1998)

9. J. Orlik

Homogenization for viscoelasticity of the integral type with aging and shrinkage

A multiphase composite with periodic distributed inclusions with a smooth boundary is considered in this contribution. The composite component materials are supposed to be linear viscoelastic and aging (of the non-convolution integral type, for which the Laplace transform with respect to time is not effectively applicable) and are subjected to isotropic shrinkage. The free shrinkage deformation can be considered as a fictitious temperature deformation in the behavior law. The procedure presented in this paper proposes a way to determine average (effective homogenized) viscoelastic and shrinkage (temperature) composite properties and the homogenized stressfield from known properties of the components. This is done by the extension of the asymptotic homogenization technique known for pure elastic nonhomogeneous bodies to the nonhomogeneous thermoviscoelasticity of the integral nonconvolution type. Up to now, the homogenization theory has not covered viscoelasticity of the integral type. SanchezPalencia (1980), Francfort & Suquet (1987) (see [2], [9]) have considered homogenization for viscoelasticity of the differential form and only up to the first derivative order. The integralmodeled viscoelasticity is more general then the differential one and includes almost all known differential models. The homogenization procedure is based on the construction of an asymptotic solution with respect to a period of the composite structure. This reduces the original problem to some auxiliary boundary value problems of elasticity and viscoelasticity on the unit periodic cell, of the same type as the original non-homogeneous problem. The existence and uniqueness results for such problems were obtained for kernels satisfying some constrain conditions. This is done by the extension of the Volterra integral operator theory to the Volterra operators with respect to the time, whose 1 kernels are space linear operators for any fixed time variables. Some ideas of such approach were proposed in [11] and [12], where the Volterra operators with kernels depending additionally on parameter were considered. This manuscript delivers results of the same nature for the case of the spaceoperator kernels.
(20 pages, 1998)

10. J. Mohring

Helmholtz Resonators with Large Aperture

The lowest resonant frequency of a cavity resonator is usually approximated by the classical Helmholtz formula. However, if the opening is rather large and the front wall is narrow this formula is no longer valid. Here we present a correction which is of third order in the ratio of the diameters of aperture and cavity. In addition to the high accuracy it allows to estimate the damping due to radiation. The result is found by applying the method of matched asymptotic expansions. The correction contains form factors describing the shapes of opening and cavity. They are computed for a number of standard geometries. Results are compared with numerical computations.
(21 pages, 1998)

11. H. W. Hamacher, A. Schöbel

On Center Cycles in Grid Graphs

Finding "good" cycles in graphs is a problem of great interest in graph theory as well as in locational analysis. We show that the center and median problems are NP hard in general graphs. This result holds both for the variable cardinality case (i.e. all cycles of the graph are considered) and the fixed cardinality case (i.e. only cycles with a given cardinality p are feasible). Hence it is of interest to investigate special cases where the problem is solvable in polynomial time. In grid graphs, the variable cardinality case is, for instance, trivially solvable if the shape of the cycle can be chosen freely. If the shape is fixed to be a rectangle one can analyze rectangles in grid graphs with, in sequence, fixed dimension, fixed cardinality, and variable cardinality. In all cases a complete characterization of the optimal cycles and closed form expressions of the optimal objective values are given, yielding polynomial time algorithms for all cases of center rectangle problems. Finally, it is shown that center cycles can be chosen as rectangles for small cardinalities such that the center cycle problem in grid graphs is in these cases completely solved.
(15 pages, 1998)

12. H. W. Hamacher, K.-H. Küfer

Inverse radiation therapy planning - a multiple objective optimisation approach

For some decades radiation therapy has been proved successful in cancer treatment. It is the major task of clinical radiation treatment planning to realize on the one hand a high level dose of radiation in the cancer tissue in order to obtain maximum tumor control. On the other hand it is obvious that it is absolutely necessary to keep in the tissue outside the tumor, particularly in organs at risk, the unavoidable radiation as low as possible.

No doubt, these two objectives of treatment planning - high level dose in the tumor, low radiation outside the tumor - have a basically contradictory nature. Therefore, it is no surprise that inverse mathematical models with dose distribution bounds tend to be infeasible in most cases. Thus, there is need for approximations compromising between overdosing the organs at risk and underdosing the target volume.

Differing from the currently used time consuming iterative approach, which measures deviation from an ideal (non-achievable) treatment plan using recursively trial-and-error weights for the organs of interest, we go a new way trying to avoid a priori weight choices and consider the treatment planning problem as a multiple objective linear programming problem: with each organ of interest, target tissue as well as organs at risk, we associate an objective function measuring the maximal deviation from the prescribed doses.

We build up a data base of relatively few efficient solutions representing and approximating the variety of Pareto solutions of the multiple objective linear programming problem. This data base can be easily scanned by physicians looking for an adequate treatment plan with the aid of an appropriate online tool.
(14 pages, 1999)

13. C. Lang, J. Ohser, R. Hilfer

On the Analysis of Spatial Binary Images

This paper deals with the characterization of microscopically heterogeneous, but macroscopically homogeneous spatial structures. A new method is presented which is strictly based on integral-geometric formulae such as Crofton's intersection formulae and Hadwiger's recursive definition of the Euler number. The corresponding algorithms have clear advantages over other techniques. As an example of application we consider the analysis of spatial digital images produced by means of Computer Assisted Tomography.
(20 pages, 1999)

14. M. Junk

On the Construction of Discrete Equilibrium Distributions for Kinetic Schemes

A general approach to the construction of discrete equilibrium distributions is presented. Such distribution functions can be used to set up Kinetic Schemes as well as Lattice Boltzmann methods. The general principles are also applied to the construction of Chapman Enskog distributions which are used in Kinetic Schemes for compressible Navier-Stokes equations.
(24 pages, 1999)

15. M. Junk, S. V. Raghurame Rao

A new discrete velocity method for Navier-Stokes equations

The relation between the Lattice Boltzmann Method, which has recently become popular, and the Kinetic Schemes, which are routinely used in Computational Fluid Dynamics, is explored. A new discrete velocity model for the numerical solution of Navier-Stokes equations for incompressible fluid flow is presented by combining both the approaches. The new scheme can be interpreted as a pseudo-compressibility method and, for a particular choice of parameters, this interpretation carries over to the Lattice Boltzmann Method.
(20 pages, 1999)

16. H. Neunzert

Mathematics as a Key to Key Technologies

The main part of this paper will consist of examples, how mathematics really helps to solve industrial problems; these examples are taken from our Institute for Industrial Mathematics, from research in the Technomathematics group at my university, but also from ECMI groups and a company called TecMath, which originated 10 years ago from my university group and has already a very successful history.
(39 pages (4 PDF-Files), 1999)

17. J. Ohser, K. Sandau

Considerations about the Estimation of the Size Distribution in Wicksell's Corpuscle Problem

Wicksell's corpuscle problem deals with the estimation of the size distribution of a population of particles, all having the same shape, using a lower dimensional sampling probe. This problem was originary formulated for particle systems occurring in life sciences but its solution is of actual and increasing interest in materials science. From a mathematical point of view, Wicksell's problem is an inverse problem where the interesting size distribution is the unknown part of a Volterra equation. The problem is often regarded ill-posed, because the structure of the integrand implies unstable numerical solutions. The accuracy of the numerical solutions is considered here using the condition number, which allows to compare different numerical methods with different (equidistant) class sizes and which indicates, as one result, that a finite section thickness of the probe reduces the numerical problems. Furthermore, the relative error of estimation is computed which can be split into two parts. One part consists of the relative discretization error that increases for increasing class size, and the second part is related to the relative statistical error which increases with decreasing class size. For both parts, upper bounds can be given and the sum of them indicates an optimal class width depending on some specific constants.
(18 pages, 1999)

18. E. Carrizosa, H. W. Hamacher, R. Klein, S. Nickel

Solving nonconvex planar location problems by finite dominating sets

It is well-known that some of the classical location problems with polyhedral gauges can be solved in polynomial time by finding a finite dominating set, i. e. a finite set of candidates guaranteed to contain at least one optimal location.

In this paper it is first established that this result holds for a much larger class of problems than currently considered in the literature. The model for which this result can be proven includes, for instance, location problems with attraction and repulsion, and location-allocation problems.

Next, it is shown that the approximation of general gauges by polyhedral ones in the objective function of our general model can be analyzed with regard to the subsequent error in the optimal objective value. For the approximation problem two different approaches are described, the sandwich procedure and the greedy algorithm. Both of these approaches lead - for fixed epsilon - to polynomial approximation algorithms with accuracy epsilon for solving the general model considered in this paper.

Keywords: Continuous Location, Polyhedral Gauges, Finite Dominating Sets, Approximation, Sandwich Algorithm, Greedy Algorithm
(19 pages, 2000)

19. A. Becker

A Review on Image Distortion Measures

Within this paper we review image distortion measures. A distortion measure is a criterion that assigns a "quality number" to an image. We distinguish between mathematical distortion measures and those distortion measures in-cooperating a priori knowledge about the imaging devices (e. g. satellite images), image processing algorithms or the human physiology. We will consider representative examples of different kinds of distortion measures and are going to discuss them.

Keywords: Distortion measure, human visual system
(26 pages, 2000)

20. H. W. Hamacher, M. Labbé, S. Nickel, T. Sonneborn

Polyhedral Properties of the Uncapacitated Multiple Allocation Hub Location Problem

We examine the feasibility polyhedron of the uncapacitated hub location problem (UHL) with multiple allocation, which has applications in the fields of air passenger and cargo transportation, telecommunication and postal delivery services. In particular we determine the dimension and derive some classes of facets of this polyhedron. We develop some general rules about lifting facets from the uncapacitated facility location (UFL) for UHL and projecting facets from UHL to UFL. By applying these rules we get a new class of facets for UHL which dominates the inequalities in the original formulation. Thus we get a new formulation of UHL whose constraints are all facet–defining. We show its superior computational performance by benchmarking it on a well known data set.

Keywords: integer programming, hub location, facility location, valid inequalities, facets, branch and cut
(21 pages, 2000)

21. H. W. Hamacher, A. Schöbel

Design of Zone Tariff Systems in Public Transportation

Given a public transportation system represented by its stops and direct connections between stops, we consider two problems dealing with the prices for the customers: The fare problem in which subsets of stops are already aggregated to zones and "good" tariffs have to be found in the existing zone system. Closed form solutions for the fare problem are presented for three objective functions. In the zone problem the design of the zones is part of the problem. This problem is NP hard and we therefore propose three heuristics which prove to be very successful in the redesign of one of Germany's transportation systems.
(30 pages, 2001)

22. D. Hietel, M. Junk, R. Keck, D. Teleaga

The Finite-Volume-Particle Method for Conservation Laws

In the Finite-Volume-Particle Method (FVPM), the weak formulation of a hyperbolic conservation law is discretized by restricting it to a discrete set of test functions. In contrast to the usual Finite-Volume approach, the test functions are not taken as characteristic functions of the control volumes in a spatial grid, but are chosen from a partition of unity with smooth and overlapping partition functions (the particles), which can even move along pre- scribed velocity fields. The information exchange between particles is based on standard numerical flux functions. Geometrical information, similar to the surface area of the cell faces in the Finite-Volume Method and the corresponding normal directions are given as integral quantities of the partition functions. After a brief derivation of the Finite-Volume-Particle Method, this work focuses on the role of the geometric coefficients in the scheme.
(16 pages, 2001)

23. T. Bender, H. Hennes, J. Kalcsics, M. T. Melo, S. Nickel

Location Software and Interface with GIS and Supply Chain Management

The objective of this paper is to bridge the gap between location theory and practice. To meet this objective focus is given to the development of software capable of addressing the different needs of a wide group of users. There is a very active community on location theory encompassing many research fields such as operations research, computer science, mathematics, engineering, geography, economics and marketing. As a result, people working on facility location problems have a very diverse background and also different needs regarding the software to solve these problems. For those interested in non-commercial applications (e. g. students and researchers), the library of location algorithms (LoLA can be of considerable assistance. LoLA contains a collection of efficient algorithms for solving planar, network and discrete facility location problems. In this paper, a detailed description of the functionality of LoLA is presented. In the fields of geography and marketing, for instance, solving facility location problems requires using large amounts of demographic data. Hence, members of these groups (e. g. urban planners and sales managers) often work with geographical information too s. To address the specific needs of these users, LoLA was inked to a geographical information system (GIS) and the details of the combined functionality are described in the paper. Finally, there is a wide group of practitioners who need to solve large problems and require special purpose software with a good data interface. Many of such users can be found, for example, in the area of supply chain management (SCM). Logistics activities involved in strategic SCM include, among others, facility location planning. In this paper, the development of a commercial location software tool is also described. The too is embedded in the Advanced Planner and Optimizer SCM software developed by SAP AG, Walldorf, Germany. The paper ends with some conclusions and an outlook to future activities.

Keywords: facility location, software development, geographical information systems, supply chain management

(48 pages, 2001)

24. H. W. Hamacher, S. A. Tjandra

Mathematical Modelling of Evacuation Problems: A State of Art

This paper details models and algorithms which can be applied to evacuation problems. While it concentrates on building evacuation many of the results are applicable also to regional evacuation. All models consider the time as main parameter, where the travel time between components of the building is part of the input and the overall evacuation time is the output. The paper distinguishes between macroscopic and microscopic evacuation models both of which are able to capture the evacuees' movement over time.

Macroscopic models are mainly used to produce good lower bounds for the evacuation time and do not consider any individual behavior during the emergency situation. These bounds can be used to analyze existing buildings or help in the design phase of planning a building. Macroscopic approaches which are based on dynamic network flow models (minimum cost dynamic flow, maximum dynamic flow, universal maximum flow, quickest path and quickest flow) are described. A special feature of the presented approach is the fact, that travel times of evacuees are not restricted to be constant, but may be density dependent. Using multicriteria optimization priority regions and blockage due to fire or smoke may be considered. It is shown how the modelling can be done using time parameter either as discrete or continuous parameter.

Microscopic models are able to model the individual evacuee's characteristics and the interaction among evacuees which influence their movement. Due to the corresponding huge amount of data one uses simulation approaches. Some probabilistic laws for individual evacuee's movement are presented. Moreover ideas to model the evacuee's movement using cellular automata (CA) and resulting software are presented.

In this paper we will focus on macroscopic models and only summarize some of the results of the microscopic approach. While most of the results are applicable to general evacuation situations, we concentrate on building evacuation.

(44 pages, 2001)

25. J. Kuhnert, S. Tiwari

Grid free method for solving the Poisson equation

A Grid free method for solving the Poisson equation is presented. This is an iterative method. The method is based on the weighted least squares approximation in which the Poisson equation is enforced to be satisfied in every iterations. The boundary conditions can also be enforced in the iteration process. This is a local approximation procedure. The Dirichlet, Neumann and mixed boundary value problems on a unit square are presented and the analytical solutions are compared with the exact solutions. Both solutions matched perfectly.

Keywords: Poisson equation, Least squares method, Grid free method

(19 pages, 2001)

26. T. Götz, H. Rave, D. Reinel-Bitzer, K. Steiner, H. Tiemeier

Simulation of the fiber spinning process

To simulate the influence of process parameters to the melt spinning process a fiber model is used and coupled with CFD calculations of the quench air flow. In the fiber model energy, momentum and mass balance are solved for the polymer mass flow. To calculate the quench air the Lattice Boltzmann method is used. Simulations and experiments for different process parameters and hole configurations are compared and show a good agreement.

Keywords: Melt spinning, fiber model, Lattice Boltzmann, CFD

(19 pages, 2001)

27. A. Zemitis

On interaction of a liquid film with an obstacle

In this paper mathematical models for liquid films generated by impinging jets are discussed. Attention is stressed to the interaction of the liquid film with some obstacle. S. G. Taylor [Proc. R. Soc. London Ser. A 253, 313 (1959)] found that the liquid film generated by impinging jets is very sensitive to properties of the wire which was used as an obstacle. The aim of this presentation is to propose a modification of the Taylor's model, which allows to simulate the film shape in cases, when the angle between jets is different from 180°. Numerical results obtained by discussed models give two different shapes of the liquid film similar as in Taylors experiments. These two shapes depend on the regime: either droplets are produced close to the obstacle or not. The difference between two regimes becomes larger if the angle between jets decreases. Existence of such two regimes can be very essential for some applications of impinging jets, if the generated liquid film can have a contact with obstacles.

Keywords: impinging jets, liquid film, models, numerical solution, shape

(22 pages, 2001)

28. I. Ginzburg, K. Steiner

Free surface lattice-Boltzmann method to model the filling of expanding cavities by Bingham Fluids

The filling process of viscoplastic metal alloys and plastics in expanding cavities is modelled using the lattice Boltzmann method in two and three dimensions. These models combine the regularized Bingham model for viscoplastic with a free-interface algorithm. The latter is based on a modified immiscible lattice Boltzmann model in which one species is the fluid and the other one is considered as vacuum. The boundary conditions at the curved liquid-vacuum interface are met without any geometrical front reconstruction from a first-order Chapman-Enskog expansion. The numerical results obtained with these models are found in good agreement with available theoretical and numerical analysis.

Keywords: Generalized LBE, free-surface phenomena, interface boundary conditions, filling processes, Bingham viscoplastic model, regularized models

(22 pages, 2001)

29. H. Neunzert

»Denn nichts ist für den Menschen als Menschen etwas wert, was er nicht mit Leidenschaft tun kann«
Vortrag anlässlich der Verleihung des Akademiepreises des Landes Rheinland-Pfalz am 21.11.2001

Was macht einen guten Hochschullehrer aus? Auf diese Frage gibt es sicher viele verschiedene, fachbezogene Antworten, aber auch ein paar allgemeine Gesichtspunkte: es bedarf der »Leidenschaft« für die Forschung (Max Weber), aus der dann auch die Begeisterung für die Lehre erwächst. Forschung und Lehre gehören zusammen, um die Wissenschaft als lebendiges Tun vermitteln zu können. Der Vortrag gibt Beispiele dafür, wie in angewandter Mathematik Forschungsaufgaben aus praktischen Alltagsproblemstellungen erwachsen, die in die Lehre auf verschiedenen Stufen (Gymnasium bis Graduiertenkolleg) einfließen; er leitet damit auch zu einem aktuellen Forschungsgebiet, der Mehrskalenanalyse mit ihren vielfältigen Anwendungen in Bildverarbeitung, Materialentwicklung und Strömungsmechanik über, was aber nur kurz gestreift wird. Mathematik erscheint hier als eine moderne Schlüsseltechnologie, die aber auch enge Beziehungen zu den Geistes- und Sozialwissenschaften hat.

Keywords: Lehre, Forschung, angewandte Mathematik, Mehrskalenanalyse, Strömungsmechanik

(18 pages, 2001)

30. J. Kuhnert, S. Tiwari

Finite pointset method based on the projection method for simulations of the incompressible Navier-Stokes equations

A Lagrangian particle scheme is applied to the projection method for the incompressible Navier-Stokes equations. The approximation of spatial derivatives is obtained by the weighted least squares method. The pressure Poisson equation is solved by a local iterative procedure with the help of the least squares method. Numerical tests are performed for two dimensional cases. The Couette flow, Poiseuelle flow, decaying shear flow and the driven cavity flow are presented. The numerical solutions are obtained for stationary as well as instationary cases and are compared with the analytical solutions for channel flows. Finally, the driven cavity in a unit square is considered and the stationary solution obtained from this scheme is compared with that from the finite element method.

Keywords: Incompressible Navier-Stokes equations, Meshfree method, Projection method, Particle scheme, Least squares approximation

AMS subject classification: 76D05, 76M28

(25 pages, 2001)

31. R. Korn, M. Krekel

Optimal Portfolios with Fixed Consumption or Income Streams

We consider some portfolio optimisation problems where either the investor has a desire for an a priori specified consumption stream or/and follows a deterministic pay in scheme while also trying to maximize expected utility from final wealth. We derive explicit closed form solutions for continuous and discrete monetary streams. The mathematical method used is classical stochastic control theory.

Keywords: Portfolio optimisation, stochastic control, HJB equation, discretisation of control problems.

(23 pages, 2002)

32. M. Krekel

Optimal portfolios with a loan dependent credit spread

If an investor borrows money he generally has to pay higher interest rates than he would have received, if he had put his funds on a savings account. The classical model of continuous time portfolio optimisation ignores this effect. Since there is obviously a connection between the default probability and the total

percentage of wealth, which the investor is in debt, we study portfolio optimisation with a control dependent interest rate. Assuming a logarithmic and a power utility function, respectively, we prove explicit formulae of the optimal control.
Keywords: Portfolio optimisation, stochastic control, HJB equation, credit spread, log utility, power utility, non-linear wealth dynamics
(25 pages, 2002)

33. J. Ohser, W. Nagel, K. Schladitz

The Euler number of discretized sets - on the choice of adjacency in homogeneous lattices

Two approaches for determining the Euler-Poincaré characteristic of a set observed on lattice points are considered in the context of image analysis { the integral geometric and the polyhedral approach. Information about the set is assumed to be available on lattice points only. In order to retain properties of the Euler number and to provide a good approximation of the true Euler number of the original set in the Euclidean space, the appropriate choice of adjacency in the lattice for the set and its background is crucial. Adjacencies are defined using tessellations of the whole space into polyhedrons. In R 3 , two new 14 adjacencies are introduced additionally to the well known 6 and 26 adjacencies. For the Euler number of a set and its complement, a consistency relation holds. Each of the pairs of adjacencies (14:1; 14:1), (14:2; 14:2), (6; 26), and (26; 6) is shown to be a pair of complementary adjacencies with respect to this relation. That is, the approximations of the Euler numbers are consistent if the set and its background (complement) are equipped with this pair of adjacencies. Furthermore, sufficient conditions for the correctness of the approximations of the Euler number are given. The analysis of selected microstructures and a simulation study illustrate how the estimated Euler number depends on the chosen adjacency. It also shows that there is not a uniquely best pair of adjacencies with respect to the estimation of the Euler number of a set in Euclidean space.
Keywords: image analysis, Euler number, neighborhod relationships, cuboidal lattice
(32 pages, 2002)

34. I. Ginzburg, K. Steiner

Lattice Boltzmann Model for Free-Surface flow and Its Application to Filling Process in Casting

A generalized lattice Boltzmann model to simulate free-surface is constructed in both two and three dimensions. The proposed model satisfies the interfacial boundary conditions accurately. A distinctive feature of the model is that the collision processes is carried out only on the points occupied partially or fully by the fluid. To maintain a sharp interfacial front, the method includes an anti-diffusion algorithm. The unknown distribution functions at the interfacial region are constructed according to the first order Chapman-Enskog analysis. The interfacial boundary conditions are satisfied exactly by the coefficients in the Chapman-Enskog expansion. The distribution functions are naturally expressed in the local interfacial coordinates. The macroscopic quantities at the interface are extracted from the least-square solutions of a locally linearized system obtained from the known distribution functions. The proposed method does not require any geometric front construction and is robust for any interfacial topology. Simulation results of realistic filling process are presented: rectangular cavity in two dimensions and Hammer box, Campbell box, Sheffield box, and Motorblock in three dimensions. To enhance the stability at high Reynolds numbers, various upwind-type schemes are developed. Free-slip and no-slip boundary conditions are also discussed.
Keywords: Lattice Boltzmann models; free-surface phenomena; interface boundary conditions; filling processes; injection molding; volume of fluid method; interface boundary conditions; advection-schemes; upwind-schemes
(54 pages, 2002)

35. M. Günther, A. Klar, T. Materne, R. Wegener

Multivalued fundamental diagrams and stop and go waves for continuum traffic equations

In the present paper a kinetic model for vehicular traffic leading to multivalued fundamental diagrams is developed and investigated in detail. For this model phase transitions can appear depending on the local density and velocity of the flow. A derivation of associated macroscopic traffic equations from the kinetic equation is given. Moreover, numerical experiments show the appearance of stop and go waves for highway traffic with a bottleneck.
Keywords: traffic flow, macroscopic equations, kinetic derivation, multivalued fundamental diagram, stop and go waves, phase transitions
(25 pages, 2002)

36. S. Feldmann, P. Lang, D. Prätzel-Wolters

Parameter influence on the zeros of network determinants

To a network N(q) with determinant D(s;q) depending on a parameter vector q Î Rr via identification of some of its vertices, a network N^ (q) is assigned. The paper deals with procedures to find N^ (q), such that its determinant D^ (s;q) admits a factorization in the determinants of appropriate subnetworks, and with the estimation of the deviation of the zeros of D^ from the zeros of D. To solve the estimation problem state space methods are applied.
Keywords: Networks, Equicofactor matrix polynomials, Realization theory, Matrix perturbation theory
(30 pages, 2002)

37. K. Koch, J. Ohser, K. Schladitz

Spectral theory for random closed sets and estimating the covariance via frequency space

A spectral theory for stationary random closed sets is developed and provided with a sound mathematical basis. Definition and proof of existence of the Bartlett spectrum of a stationary random closed set as well as the proof of a Wiener-Khintchine theorem for the power spectrum are used to two ends: First, well known second order characteristics like the covariance can be estimated faster than usual via frequency space. Second, the Bartlett spectrum and the power spectrum can be used as second order characteristics in frequency space. Examples show, that in some cases information about the random closed set is easier to obtain from these characteristics in frequency space than from their real world counterparts.
Keywords: Random set, Bartlett spectrum, fast Fourier transform, power spectrum
(28 pages, 2002)

38. D. d'Humières, I. Ginzburg

Multi-reflection boundary conditions for lattice Boltzmann models

We present a unified approach of several boundary conditions for lattice Boltzmann models. Its general framework is a generalization of previously introduced schemes such as the bounce-back rule, linear or quadratic interpolations, etc. The objectives are two fold: first to give theoretical tools to study the existing boundary conditions and their corresponding accuracy; secondly to design formally third- order accurate boundary conditions for general flows. Using these boundary conditions, Couette and Poiseuille flows are exact solution of the lattice Boltzmann models for a Reynolds number Re = 0 (Stokes limit).
Numerical comparisons are given for Stokes flows in periodic arrays of spheres and cylinders, linear periodic array of cylinders between moving plates and for Navier-Stokes flows in periodic arrays of cylinders for Re < 200. These results show a significant improvement of the overall accuracy when using the linear interpolations instead of the bounce-back reflection (up to an order of magnitude on the hydrodynamics fields). Further improvement is achieved with the new multi-reflection boundary conditions, reaching a level of accuracy close to the quasi-analytical reference solutions, even for rather modest grid resolutions and few points in the narrowest channels. More important, the pressure and velocity fields in the vicinity of the obstacles are much smoother with multi-reflection than with the other boundary conditions.
Finally the good stability of these schemes is highlighted by some simulations of moving obstacles: a cylinder between flat walls and a sphere in a cylinder.
Keywords: lattice Boltzmann equation, boudary condistions, bounce-back rule, Navier-Stokes equation
(72 pages, 2002)

39. R. Korn

Elementare Finanzmathematik

Im Rahmen dieser Arbeit soll eine elementar gehaltene Einführung in die Aufgabenstellungen und Prinzipien der modernen Finanzmathematik gegeben werden. Insbesondere werden die Grundlagen der Modellierung von Aktienkursen, der Bewertung von Optionen und der Portfolio-Optimierung vorgestellt. Natürlich können die verwendeten Methoden und die entwickelte Theorie nicht in voller Allgemeinheit für den Schulunterricht verwendet werden, doch sollen einzelne Prinzipien so heraus gearbeitet werden, dass sie auch an einfachen Beispielen verstanden werden können.
Keywords: Finanzmathematik, Aktien, Optionen, Portfolio-Optimierung, Börse, Lehrerweiterbildung, Mathematikunterricht
(98 pages, 2002)

40. J. Kallrath, M. C. Müller, S. Nickel

Batch Presorting Problems: Models and Complexity Results

In this paper we consider short term storage systems. We analyze presorting strategies to improve the effiency of these storage systems. The presorting task is called Batch PreSorting Problem (BPSP). The BPSP is a variation of an assigment problem, i. e., it has an assigment problem kernel and some additional constraints. We present different types of these presorting problems, introduce mathematical programming formulations and prove the NP-completeness for one type of the BPSP. Experiments are carried out in order to compare the different model formulations and to investigate the behavior of these models.
Keywords: Complexity theory, Integer programming, Assigment, Logistics
(19 pages, 2002)

41. J. Linn

On the frame-invariant description of the phase space of the Folgar-Tucker equation

The Folgar-Tucker equation is used in flow simulations of fiber suspensions to predict fiber orientation depending on the local flow. In this paper, a complete, frame-invariant description of the phase space of this differential equation is presented for the first time.
Key words: fiber orientation, Folgar-Tucker equation, injection molding
(5 pages, 2003)

42. T. Hanne, S. Nickel

A Multi-Objective Evolutionary Algorithm for Scheduling and Inspection Planning in Software Development Projects

In this article, we consider the problem of planning inspections and other tasks within a software development (SD) project with respect to the objectives quality (no. of defects), project duration, and costs. Based on a discrete-event simulation model of SD processes comprising the phases coding, inspection, test, and rework, we present a simplified formulation of the problem as a multiobjective optimization problem. For solving the problem (i. e. finding an approximation of the efficient set) we develop a multiobjective evolutionary algorithm. Details of the algorithm are discussed as well as results of its application to sample problems.
Key words: multiple objective programming, project management and scheduling, software development, evolutionary algorithms, efficient set
(29 pages, 2003)

43. T. Bortfeld , K.-H. Küfer, M. Monz, A. Scherrer, C. Thieke, H. Trinkaus

Intensity-Modulated Radiotherapy - A Large Scale Multi-Criteria Programming Problem -

Radiation therapy planning is always a tight rope walk between dangerous insufficient dose in the target volume and life threatening overdosing of organs at risk. Finding ideal balances between these inherently contradictory goals challenges dosimetrists and physicians in their daily practice. Today's planning systems are typically based on a single evaluation function that measures the quality of a radiation treatment plan. Unfortunately, such a one dimensional approach cannot satisfactorily map the different backgrounds of physicians and the patient dependent necessities. So, too often a time consuming iteration process between evaluation of dose distribution and redefinition of the evaluation function is needed.
In this paper we propose a generic multi-criteria approach based on Pareto's solution concept. For each entity of interest - target volume or organ at risk a structure dependent evaluation function is defined measuring deviations from ideal doses that are calculated from statistical functions. A reasonable bunch of clinically meaningful Pareto optimal solutions are stored in a data base, which can be interactively searched by physicians. The system guarantees dynamical planning as well as the discussion of tradeoffs between different entities.
Mathematically, we model the upcoming inverse problem as a multi-criteria linear programming problem. Because of the large scale nature of the problem it is not possible to solve the problem in a 3D-setting without adaptive reduction by appropriate approximation schemes.
Our approach is twofold: First, the discretization of the continuous problem is based on an adaptive hierarchical clustering process which is used for a local refinement of constraints during the optimization procedure. Second, the set of Pareto optimal solutions is approximated by an adaptive grid of representatives that are found by a hybrid process of calculating extreme compromises and interpolation methods.
Keywords: multiple criteria optimization, representative systems of Pareto solutions, adaptive triangulation, clustering and disaggregation techniques, visualization of Pareto solutions, medical physics, external beam radiotherapy planning, intensity modulated radiotherapy
(31 pages, 2003)

44. T. Halfmann, T. Wichmann

Overview of Symbolic Methods in Industrial Analog Circuit Design

Industrial analog circuits are usually designed using numerical simulation tools. To obtain a deeper circuit understanding, symbolic analysis techniques can additionally be applied. Approximation methods which reduce the complexity of symbolic expressions are needed in order to handle industrial-sized problems. This paper will give an overview to the field of symbolic analog circuit analysis. Starting with a motivation, the state-of-the-art simplification algorithms for linear as well as for nonlinear circuits are presented. The basic ideas behind the different techniques are described, whereas the technical details can be found in the cited references. Finally, the application of linear and nonlinear symbolic analysis will be shown on two example circuits.
Keywords: CAD, automated analog circuit design, symbolic analysis, computer algebra, behavioral modeling, system simulation, circuit sizing, macro modeling, differential-algebraic equations, index
(17 pages, 2003)

45. S. E. Mikhailov, J. Orlik

Asymptotic Homogenisation in Strength and Fatigue Durability Analysis of Composites

Asymptotic homogenisation technique and two-scale convergence is used for analysis of macro-strength and fatigue durability of composites with a periodic structure under cyclic loading. The linear damage accumulation rule is employed in the phenomenological micro-durability conditions (for each component of the composite) under varying cyclic loading. Both local and non-local strength and durability conditions are analysed. The strong convergence of the strength and fatigue damage measure as the structure period tends to zero is proved and their limiting values are estimated.
Keywords: multiscale structures, asymptotic homogenization, strength, fatigue, singularity, non-local conditions
(14 pages, 2003)

46. P. Domínguez-Marín, P. Hansen, N. Mladenovi´c , S. Nickel

Heuristic Procedures for Solving the Discrete Ordered Median Problem

We present two heuristic methods for solving the Discrete Ordered Median Problem (DOMP), for which no such approaches have been developed so far. The DOMP generalizes classical discrete facility location problems, such as the p-median, p-center and Uncapacitated Facility Location problems. The first procedure proposed in this paper is based on a genetic algorithm developed by Moreno Vega [MV96] for p-median and p-center problems. Additionally, a second heuristic approach based on the Variable Neighborhood Search metaheuristic (VNS) proposed by Hansen & Mladenovic [HM97] for the p-median problem is described. An extensive numerical study is presented to show the efficiency of both heuristics and compare them.
Keywords: genetic algorithms, variable neighborhood search, discrete facility location
(31 pages, 2003)

47. N. Boland, P. Domínguez-Marín, S. Nickel, J. Puerto

Exact Procedures for Solving the Discrete Ordered Median Problem

The Discrete Ordered Median Problem (DOMP) generalizes classical discrete location problems, such as the N-median, N-center and Uncapacitated Facility Location problems. It was introduced by Nickel [16], who formulated it as both a nonlinear and a linear integer program. We propose an alternative integer linear programming formulation for the DOMP, discuss relationships between both integer linear programming formulations, and show how properties of optimal solutions can be used to strengthen these formulations. Moreover, we present a specific branch and bound procedure to solve the DOMP more efficiently. We test the integer linear programming formulations and this branch and bound method computationally on randomly generated test problems.
Keywords: discrete location, Integer programming
(41 pages, 2003)

48. S. Feldmann, P. Lang

Padé-like reduction of stable discrete linear systems preserving their stability

A new stability preserving model reduction algorithm for discrete linear SISO-systems based on their impulse response is proposed. Similar to the Padé approximation, an equation system for the Markov parameters involving the Hankel matrix is considered, that here however is chosen to be of very high dimension. Although this equation system therefore in general cannot be solved exactly, it is proved that the approximate solution, computed via the Moore-Penrose inverse, gives rise to a stability preserving reduction scheme, a property that cannot be guaranteed for the Padé approach. Furthermore, the proposed algorithm is compared to another stability preserving reduction approach, namely the balanced truncation method, showing comparable performance of the reduced systems. The balanced truncation method however starts from a state space description of the systems and in general is expected to be more computational demanding.
Keywords: Discrete linear systems, model reduction, stability, Hankel matrix, Stein equation
(16 pages, 2003)

49. J. Kallrath, S. Nickel

A Polynomial Case of the Batch Presorting Problem

This paper presents new theoretical results for a special case of the batch presorting problem (BPSP). We will show tht this case can be solved in polynomial time. Offline and online algorithms are presented for solving the BPSP. Competetive analysis is used for comparing the algorithms.
Keywords: batch presorting problem, online optimization, competetive analysis, polynomial algorithms, logistics
(17 pages, 2003)

50. T. Hanne, H. L. Trinkaus

knowCube for MCDM – Visual and Interactive Support for Multicriteria Decision Making

In this paper, we present a novel multicriteria decision support system (MCDSS), called knowCube, consisting of components for knowledge organization, generation, and navigation. Knowledge organization rests upon a database for managing qualitative and quantitative criteria, together with add-on information. Knowledge generation serves filling the database via e. g. identification, optimization, classification or simulation. For "finding needles in haycocks", the knowledge navigation component supports graphical database retrieval and interactive, goal-oriented problem solving. Navigation "helpers" are, for instance, cascading criteria aggregations, modifiable metrics, ergonomic interfaces, and customizable visualizations. Examples from real-life projects, e.g. in industrial engineering and in the life sciences, illustrate the application of our MCDSS.
Key words: Multicriteria decision making, knowledge management, decision support systems, visual interfaces, interactive navigation, real-life applications.
(26 pages, 2003)

51. O. Iliev, V. Laptev

On Numerical Simulation of Flow Through Oil Filters

This paper concerns numerical simulation of flow through oil filters. Oil filters consist of filter housing (filter box), and a porous filtering medium, which completely separates the inlet from the outlet. We discuss mathematical models, describing coupled flows in the pure liquid subregions and in the porous filter media, as well as interface conditions between them. Further, we reformulate the problem in fictitious regions method manner, and discuss peculiarities of the numerical algorithm in solving the coupled system. Next, we show numerical results, validating the model and the algorithm. Finally, we present results from simulation of 3-D oil flow through a real car filter.
Keywords: oil filters, coupled flow in plain and porous media, Navier-Stokes, Brinkman, numerical simulation
(8 pages, 2003)

52. W. Dörfler, O. Iliev, D. Stoyanov, D. Vassileva

On a Multigrid Adaptive Refinement Solver for Saturated Non-Newtonian Flow in Porous Media

A multigrid adaptive refinement algorithm for non-Newtonian flow in porous media is presented. The saturated flow of a non-Newtonian fluid is described by the continuity equation and the generalized Darcy law. The resulting second order nonlinear elliptic equation is discretized by a finite volume method on a cell-centered grid. A nonlinear full-multigrid, full-approximation-storage algorithm is implemented. As a smoother, a single grid solver based on Picard linearization and Gauss-Seidel relaxation is used. Further, a local refinement multigrid algorithm on a composite grid is developed. A residual based error indicator is used in the adaptive refinement criterion. A special implementation approach is used, which allows us to perform unstructured local refinement in conjunction with the finite volume discretization. Several results from numerical experiments are presented in order to examine the performance of the solver.
Keywords: Nonlinear multigrid, adaptive refinement, non-Newtonian flow in porous media
(17 pages, 2003)

53. S. Kruse

On the Pricing of Forward Starting Options under Stochastic Volatility

We consider the problem of pricing European forward starting options in the presence of stochastic volatility. By performing a change of measure using the asset price at the time of strike determination as a numeraire, we derive a closed-form solution based on Heston's model of stochastic volatility.

Keywords: Option pricing, forward starting options, Heston model, stochastic volatility, cliquet options

(11 pages, 2003)

54. O. Iliev, D. Stoyanov

Multigrid – adaptive local refinement solver for incompressible flows

A non-linear multigrid solver for incompressible Navier-Stokes equations, exploiting finite volume discretization of the equations, is extended by adaptive local refinement. The multigrid is the outer iterative cycle, while the SIMPLE algorithm is used as a smoothing procedure. Error indicators are used to define the refinement subdomain. A special implementation approach is used, which allows to perform unstructured local refinement in conjunction with the finite volume discretization. The multigrid - adaptive local refinement algorithm is tested on 2D Poisson equation and further is applied to a lid-driven flows in a cavity (2D and 3D case), comparing the results with bench-mark data. The software design principles of the solver are also discussed.

Keywords: Navier-Stokes equations, incompressible flow, projection-type splitting, SIMPLE, multigrid methods, adaptive local refinement, lid-driven flow in a cavity

(37 pages, 2003)

55. V. Starikovicius

The multiphase flow and heat transfer in porous media

In first part of this work, summaries of traditional Multiphase Flow Model and more recent Multiphase Mixture Model are presented. Attention is being paid to attempts include various heterogeneous aspects into models. In second part, MMM based differential model for two-phase immiscible flow in porous media is considered. A numerical scheme based on the sequential solution procedure and control volume based finite difference schemes for the pressure and saturation-conservation equations is developed. A computer simulator is built, which exploits object-oriented programming techniques. Numerical result for several test problems are reported.

Keywords: Two-phase flow in porous media, various formulations, global pressure, multiphase mixture model, numerical simulation

(30 pages, 2003)

56. P. Lang, A. Sarishvili, A. Wirsen

Blocked neural networks for knowledge extraction in the software development process

One of the main goals of an organization developing software is to increase the quality of the software while at the same time to decrease the costs and the duration of the development process. To achieve this, various decisions e.ecting this goal before and during the development process have to be made by the managers. One appropriate tool for decision support are simulation models of the software life cycle, which also help to understand the dynamics of the software development process. Building up a simulation model requires a mathematical description of the interactions between di.erent objects involved in the development process. Based on experimental data, techniques from the .eld of knowledge discovery can be used to quantify these interactions and to generate new process knowledge based on the analysis of the determined relationships. In this paper blocked neuronal networks and related relevance measures will be presented as an appropriate tool for quanti.cation and validation of qualitatively known dependencies in the software development process.

Keywords: Blocked Neural Networks, Nonlinear Regression, Knowledge Extraction, Code Inspection

(21 pages, 2003)

57. H. Knaf, P. Lang, S. Zeiser

Diagnosis aiding in Regulation Thermography using Fuzzy Logic

The objective of the present article is to give an overview of an application of Fuzzy Logic in Regulation Thermography, a method of medical diagnosis support. An introduction to this method of the complementary medical science based on temperature measurements – so-called thermograms – is provided. The process of modelling the physician's thermogram evaluation rules using the calculus of Fuzzy Logic is explained.

Keywords: fuzzy logic,knowledge representation, expert system

(22 pages, 2003)

58. M.T. Melo, S. Nickel, F. Saldanha da Gama

Largescale models for dynamic multi-commodity capacitated facility location

In this paper we focus on the strategic design of supply chain networks. We propose a mathematical modeling framework that captures many practical aspects of network design problems simultaneously but which have not received adequate attention in the literature. The aspects considered include: dynamic planning horizon, generic supply chain network structure, external supply of materials, inventory opportunities for goods, distribution of commodities, facility configuration, availability of capital for investments, and storage limitations. Moreover, network configuration decisions concerning the gradual relocation of facilities over the planning horizon are considered. To cope with fluctuating demands, capacity expansion and reduction scenarios are also analyzed as well as modular capacity shifts. The relation of the proposed modeling framework with existing models is discussed. For problems of reasonable size we report on our computational experience with standard mathematical programming software. In particular, useful insights on the impact of various factors on network design decisions are provided.

Keywords: supply chain management, strategic planning, dynamic location, modeling

(40 pages, 2003)

59. J. Orlik

Homogenization for contact problems with periodically rough surfaces

We consider the contact of two elastic bodies with rough surfaces at the interface. The size of the micro-peaks and valleys is very small compared with the macrosize of the bodies' domains. This makes the direct application of the FEM for the calculation of the contact problem prohibitively costly. A method is developed that allows deriving a macrocontact condition on the interface. The method involves the twoscale asymptotic homogenization procedure that takes into account the microgeometry of the interface layer and the stiffnesses of materials of both domains. The macrocontact condition can then be used in a FEM model for the contact problem on the macrolevel. The averaged contact stiffness obtained allows the replacement of the interface layer in the macromodel by the macrocontact condition.

Keywords: asymptotic homogenization, contact problems

(28 pages, 2004)

60. A. Scherrer, K.-H. Küfer, M. Monz, F. Alonso, T. Bortfeld

IMRT planning on adaptive volume structures – a significant advance of computational complexity

In intensity-modulated radiotherapy (IMRT) planning the oncologist faces the challenging task of finding a treatment plan that he considers to be an ideal compromise of the inherently contradictive goals of delivering a sufficiently high dose to the target while widely sparing critical structures. The search for this a priori unknown compromise typically requires the computation of several plans, i.e. the solution of several optimization problems. This accumulates to a high computational expense due to the large scale of these problems - a consequence of the discrete problem formulation. This paper presents the adaptive clustering method as a new algorithmic concept to overcome these difficulties. The computations are performed on an individually adapted structure of voxel clusters rather than on the original voxels leading to a decisively reduced computational complexity as numerical examples on real clinical data demonstrate. In contrast to many other similar concepts, the typical trade-off between a reduction in computational complexity and a loss in exactness can be avoided: the adaptive clustering method produces the optimum of the original problem. This flexible method can be applied to both single- and multi-criteria optimization methods based on most of the convex evaluation functions used in practice.

Keywords: Intensity-modulated radiation therapy (IMRT), inverse treatment planning, adaptive volume structures, hierarchical clustering, local refinement, adaptive clustering, convex programming, mesh generation, multi-grid methods

(24 pages, 2004)

61. D. Kehrwald

Parallel lattice Boltzmann simulation of complex flows

After a short introduction to the basic ideas of lattice Boltzmann methods and a brief description of a modern parallel computer, it is shown how lattice Boltzmann schemes are successfully applied for simulating fluid flow in microstructures and calculating material properties of porous media. It is explained how lattice Boltzmann schemes compute the gradient of the velocity field without numerical differentiation. This feature is then utilised for the simulation of pseudo-plastic fluids, and numerical results are presented for a simple benchmark problem as well as for the simulation of liquid composite moulding.

Keywords: Lattice Boltzmann methods, parallel computing, microstructure simulation, virtual material design, pseudo-plastic fluids, liquid composite moulding

(12 pages, 2004)

62. O. Iliev, J. Linn, M. Moog, D. Niedziela, V. Starikovicius

On the Performance of Certain Iterative Solvers for Coupled Systems Arising in Discretization of Non-Newtonian Flow Equations

Iterative solution of large scale systems arising after discretization and linearization of the unsteady non-Newtonian Navier–Stokes equations is studied. cross WLF model is used to account for the non-Newtonian behavior of the fluid. Finite volume method is used to discretize the governing system of PDEs. Viscosity is treated explicitely (e.g., it is taken from the previous time step), while other terms are treated implicitly. Different preconditioners (block–diagonal, block–triangular, relaxed incomplete LU factorization, etc.) are used in conjunction with advanced iterative methods, namely, BiCGStab, CGS, GMRES. The action of the preconditioner in fact requires inverting different blocks. For this purpose, in addition to preconditioned BiCGStab, CGS, GMRES, we use also algebraic multigrid method (AMG). The performance of the iterative solvers is studied with respect to the number of unknowns, characteristic velocity in the basic flow, time step, deviation from Newtonian behavior, etc. Results from numerical experiments are presented and discussed.

Keywords: Performance of iterative solvers, Preconditioners, Non-Newtonian flow

(17 pages, 2004)

63. R. Ciegis, O. Iliev, S. Rief, K. Steiner

On Modelling and Simulation of Different Regimes for Liquid Polymer Moulding

In this paper we consider numerical algorithms for solving a system of nonlinear PDEs arising in modeling of liquid polymer injection. We investigate the particular case when a porous preform is located within the mould, so that the liquid polymer flows through a porous medium during the filling stage. The nonlinearity of the governing system of PDEs is due to the non-Newtonian behavior of the polymer, as well as due to the moving free boundary. The latter is related to the penetration front and a Stefan type problem is formulated to account for it. A finite-volume method is used

to approximate the given differential problem. Results of numerical experiments are presented.
We also solve an inverse problem and present algorithms for the determination of the absolute preform permeability coefficient in the case when the velocity of the penetration front is known from measurements. In both cases (direct and inverse problems) we emphasize on the specifics related to the non-Newtonian behavior of the polymer. For completeness, we discuss also the Newtonian case. Results of some experimental measurements are presented and discussed.
Keywords: Liquid Polymer Moulding, Modelling, Simulation, Infiltration, Front Propagation, non-Newtonian flow in porous media
(43 pages, 2004)

64. T. Hanne, H. Neu

Simulating Human Resources in Software Development Processes

In this paper, we discuss approaches related to the explicit modeling of human beings in software development processes. While in most older simulation models of software development processes, esp. those of the system dynamics type, humans are only represented as a labor pool, more recent models of the discrete-event simulation type require representations of individual humans. In that case, particularities regarding the person become more relevant. These individual effects are either considered as stochastic variations of productivity, or an explanation is sought based on individual characteristics, such as skills for instance. In this paper, we explore such possibilities by recurring to some basic results in psychology, sociology, and labor science. Various specific models for representing human effects in software process simulation are discussed.
Keywords: Human resource modeling, software process, productivity, human factors, learning curve
(14 pages, 2004)

65. O. Iliev, A. Mikelic, P. Popov

Fluid structure interaction problems in deformable porous media: Toward permeability of deformable porous media

In this work the problem of fluid flow in deformable porous media is studied. First, the stationary fluid-structure interaction (FSI) problem is formulated in terms of incompressible Newtonian fluid and a linearized elastic solid. The flow is assumed to be characterized by very low Reynolds number and is described by the Stokes equations. The strains in the solid are small allowing for the solid to be described by the Lame equations, but no restrictions are applied on the magnitude of the displacements leading to strongly coupled, nonlinear fluid-structure problem. The FSI problem is then solved numerically by an iterative procedure which solves sequentially fluid and solid subproblems. Each of the two subproblems is discretized by finite elements and the fluid-structure coupling is reduced to an interface boundary condition. Several numerical examples are presented and the results from the numerical computations are used to perform permeability computations for different geometries.
Keywords: fluid-structure interaction, deformable porous media, upscaling, linear elasticity, stokes, finite elements
(23 pages, 2004)

66. F. Gaspar, O. Iliev, F. Lisbona, A. Naumovich, P. Vabishchevich

On numerical solution of 1-D poroelasticity equations in a multilayered domain

Finite volume discretization of Biot system of poroelasticity in a multilayered domain is presented. Staggered grid is used in order to avoid nonphysical oscillations of the numerical solution, appearing when a collocated grid is used. Various numerical experiments are presented in order to illustrate the accuracy of the finite difference scheme. In the first group of experiments, problems having analytical solutions are solved, and the order of convergence for the velocity, the pressure, the displacements, and the stresses is analyzed. In the second group of experiments numerical solution of real problems is presented.
Keywords: poroelasticity, multilayered material, finite volume discretization, MAC type grid
(41 pages, 2004)

67. J. Ohser, K. Schladitz, K. Koch, M. Nöthe

Diffraction by image processing and its application in materials science

A spectral theory for constituents of macroscopically homogeneous random microstructures modeled as homogeneous random closed sets is developed and provided with a sound mathematical basis, where the spectrum obtained by Fourier methods corresponds to the angular intensity distribution of x-rays scattered by this constituent. It is shown that the fast Fourier transform applied to three-dimensional images of microstructures obtained by micro-tomography is a powerful tool of image processing. The applicability of this technique is is demonstrated in the analysis of images of porous media.
Keywords: porous microstructure, image analysis, random set, fast Fourier transform, power spectrum, Bartlett spectrum
(13 pages, 2004)

68. H. Neunzert

Mathematics as a Technology: Challenges for the next 10 Years

No doubt: Mathematics has become a technology in its own right, maybe even a key technology. Technology may be defined as the application of science to the problems of commerce and industry. And science? Science maybe defined as developing, testing and improving models for the prediction of system behavior; the language used to describe these models is mathematics and mathematics provides methods to evaluate these models. Here we are! Why has mathematics become a technology only recently? Since it got a tool, a tool to evaluate complex, "near to reality" models: Computer! The model may be quite old – Navier-Stokes equations describe flow behavior rather well, but to solve these equations for realistic geometry and higher Reynolds numbers with sufficient precision is even for powerful parallel computing a real challenge. Make the models as simple as possible, as complex as necessary – and then evaluate them with the help of efficient and reliable algorithms: These are genuine mathematical tasks.
Keywords: applied mathematics, technology, modelling, simulation, visualization, optimization, glass processing, spinning processes, fiber-fluid interaction, trubulence effects, topological optimization, multicriteria optimization, Uncertainty and Risk, financial mathematics, Malliavin calculus, Monte-Carlo methods, virtual material design, filtration, bio-informatics, system biology
(29 pages, 2004)

69. R. Ewing, O. Iliev, R. Lazarov, A. Naumovich

On convergence of certain finite difference discretizations for 1D poroelasticity interface problems

Finite difference discretizations of 1D poroelasticity equations with discontinuous coefficients are analyzed. A recently suggested FD discretization of poroelasticity equations with constant coefficients on staggered grid, [5], is used as a basis. A careful treatment of the interfaces leads to harmonic averaging of the discontinuous coefficients. Here, convergence for the pressure and for the displacement is proven in certain norms for the scheme with harmonic averaging (HA). Order of convergence 1.5 is proven for arbitrary located interface, and second order convergence is proven for the case when the interface coincides with a grid node. Furthermore, following the ideas from [3], modified HA discretization are suggested for particular cases. The velocity and the stress are approximated with second order on the interface in this case. It is shown that for wide class of problems, the modified discretization provides better accuracy. Second order convergence for modified scheme is proven for the case when the interface coincides with a displacement grid node. Numerical experiments are presented in order to illustrate our considerations.
Keywords: poroelasticity, multilayered material, finite volume discretizations, MAC type grid, error estimates
(26 pages,2004)

70. W. Dörfler, O. Iliev, D. Stoyanov, D. Vassileva

On Efficient Simulation of Non-Newtonian Flow in Saturated Porous Media with a Multigrid Adaptive Refinement Solver

Flow of non-Newtonian in saturated porous media can be described by the continuity equation and the generalized Darcy law. Efficient solution of the resulting second order nonlinear elliptic equation is discussed here. The equation is discretized by a finite volume method on a cell-centered grid. Local adaptive refinement of the grid is introduced in order to reduce the number of unknowns. A special implementation approach is used, which allows us to perform unstructured local refinement in conjunction with the finite volume discretization. Two residual based error indicators are exploited in the adaptive refinement criterion. Second order accurate discretization on the interfaces between refined and non-refined subdomains, as well as on the boundaries with Dirichlet boundary condition, are presented here, as an essential part of the accurate and efficient algorithm. A nonlinear full approximation storage multigrid algorithm is developed especially for the above described composite (coarse plus locally refined) grid approach. In particular, second order approximation around interfaces is a result of a quadratic approximation of slave nodes in the multigrid - adaptive refinement (MG-AR) algorithm. Results from numerical solution of various academic and practice-induced problems are presented and the performance of the solver is discussed.
Keywords: Nonlinear multigrid, adaptive renement, non-Newtonian in porous media
(25 pages, 2004)

71. J. Kalcsics, S. Nickel, M. Schröder

Towards a Unified Territory Design Approach – Applications, Algorithms and GIS Integration

Territory design may be viewed as the problem of grouping small geographic areas into larger geographic clusters called territories in such a way that the latter are acceptable according to relevant planning criteria. In this paper we review the existing literature for applications of territory design problems and solution approaches for solving these types of problems. After identifying features common to all applications we introduce a basic territory design model and present in detail two approaches for solving this model: a classical location–allocation approach combined with optimal split resolution techniques and a newly developed computational geometry based method. We present computational results indicating the efficiency and suitability of the latter method for solving large–scale practical problems in an interactive environment. Furthermore, we discuss extensions to the basic model and its integration into Geographic Information Systems.
Keywords: territory desgin, political districting, sales territory alignment, optimization algorithms, Geographical Information Systems
(40 pages, 2005)

72. K. Schladitz, S. Peters, D. Reinel-Bitzer, A. Wiegmann, J. Ohser

Design of acoustic trim based on geometric modeling and flow simulation for non-woven

In order to optimize the acoustic properties of a stacked fiber non-woven, the microstructure of the non-woven is modeled by a macroscopically homogeneous random system of straight cylinders (tubes). That is, the fibers are modeled by a spatially stationary random system of lines (Poisson line process), dilated by a sphere. Pressing the non-woven causes anisotropy. In our model, this anisotropy is described by a one parametric distribution of the direction of the fibers. In the present application, the anisotropy parameter has to be estimated from 2d reflected light microscopic images of microsections of the non-woven.
After fitting the model, the flow is computed in digitized realizations of the stochastic geometric model using the lattice Boltzmann method. Based on the flow resistivity, the formulas of Delany and Bazley predict the frequency-dependent acoustic absorption of the non-woven in the impedance tube.

Using the geometric model, the description of a non-woven with improved acoustic absorption properties is obtained in the following way: First, the fiber thicknesses, porosity and anisotropy of the fiber system are modified. Then the flow and acoustics simulations are performed in the new sample. These two steps are repeatedc for various sets of parameters. Finally, the set of parameters for the geometric model leading to the best acoustic absorption is chosen.
Keywords: random system of fibers, Poisson line process, flow resistivity, acoustic absorption, Lattice-Boltzmann method, non-woven
(21 pages, 2005)

Status quo: February 2005